Lithos 258–259 (2016) 115–132

Contents lists available at ScienceDirect

Lithos

journal homepage: www.elsevier.com/locate/lithos

Invited review article

Basaltic rocks from the Andean Southern Volcanic Zone: Insights from the comparison of along-strike and small-scale geochemical variations and their sources

Rosemary Hickey-Vargas [a,*], Sven Holbik [a], Daniel Tormey [b], Frederick A. Frey [c], Hugo Moreno Roa [d,e]

[a] Department of Earth and Environment, Florida International University, Miami, FL 33199, USA
[b] ENVIRON, Los Angeles, CA 90017, USA
[c] Department of Earth, Atmospheric and Planetary Science, Massachusetts Institute of Technology, Cambridge, MA 02139, USA
[d] Departamento de Geología y Geofísica, Universidad de Chile, Santiago, Chile
[e] SERNAGEOMIN, Puerto Varas, Chile

ARTICLE INFO

Article history:
Received 11 November 2015
Accepted 8 April 2016
Available online 21 April 2016

Keywords:
Continental arc magmatism
Andean Southern Volcanic Zone
Subduction zone processes
Isotope geochemistry
Trace element geochemistry
Liquiñe–Ofqui Fault System

ABSTRACT

The origin of spatial variations in the geochemical characteristics of volcanic rocks erupted in the Andean Southern Volcanic Zone (SVZ) has been studied by numerous researchers over the past 40 years. Diverse interpretations for along-strike, across-strike, and small-scale variations have been proposed. In this paper, we review geochemical data showing along-strike geochemical variations and address the processes causing such trends. We compare large- and small-scale changes of the same geochemical parameters in basaltic rocks in order to use spatial scale as a tool for isolating processes that may have the same result. Along-strike geochemical variations in the SVZ are expected, due to 1) greater thickness or age of the sub-arc continental crust and mantle lithosphere in the Northern SVZ (NSVZ; 33°S–34°30′S) and Transitional SVZ (TSVZ; 34°30′S–37°S) compared with the Central SVZ (CSVZ; 37°S–41.5°S) and Southern SVZ (SSVZ: 41.5°S–46°S); and 2) along-strike changes of the subducting Nazca plate and overlying asthenosphere. Basalts and basaltic andesites erupted at volcanic front stratovolcanoes define several along-strike geochemical trends: 1) higher $^{87}Sr/^{86}Sr$ and lower $^{143}Nd/^{144}Nd$ at volcanoes in the NSVZ compared with the TSVZ, CSVZ, and SSVZ; 2) higher and more variable La/Yb at volcanoes in the NSVZ and TSVZ compared with the CSVZ and SSVZ; 3) lower $^{87}Sr/^{86}Sr$ for a given $^{143}Nd/^{144}Nd$ at volcanoes in the TSVZ compared with the CSVZ and SSVZ; and 4) large values for time-sensitive subduction tracers such as $^{10}Be/^{9}Be$ and $(^{238}U/^{230}Th)$ at some volcanoes in the CSVZ, but not in the NSVZ and TSVZ. Geochemical parameters that distinguish the TSVZ from the CSVZ and SSVZ are also found within the CSVZ at small basaltic eruptive centers (SEC) aligned with the Liquiñe–Ofqui Fault System (LOFS), which extends from 38°S to the southernmost SVZ. Our interpretation is that CSVZ magmas with strong time-sensitive subduction tracers represent the ambient subduction-modified asthenosphere beneath the SVZ and that TSVZ magmas and some SEC in the CSVZ are modified by interaction with pyroxenite during ascent through the mantle lithosphere. In the CSVZ and probably the SSVZ, enhanced crustal permeability created by the LOFS allows the eruption of geochemically diverse magmas on a small scale. In the TSVZ and the NSVZ, the composition of magma from the subduction-modified asthenosphere is overprinted by interaction with the mantle lithosphere.

Contents

1. Introduction . . . 116
2. Geologic background . . . 116
   2.1. Characteristics of the Nazca plate and Peru–Chile trench . . . 116
   2.2. Characteristics of the continental crust . . . 116
   2.3. Inferences about the mantle wedge . . . 118
3. Geochemical and petrologic background . . . 118
   3.1. Review of geochemical and petrologic studies delineating along-strike trends . . . 118
      3.1.1. Segments of the SVZ . . . 118
      3.1.2. Along-strike geochemical variations . . . 118

* Corresponding author at: Department of Earth and Environment, AHC5-394, Florida International University, Miami, FL 33199, USA.
E-mail address: hickey@fiu.edu (R. Hickey-Vargas).

http://dx.doi.org/10.1016/j.lithos.2016.04.014
0024-4937/

3.2. Re-examination of trends . . . 119
3.2.1. Definition of petrologic character . . . 119
3.2.2. Large-scale along-strike variations . . . 120
4. Discussion . . . 120
4.1. Along-strike variation of SiO_2 and REE . . . 120
4.1.1. The role of hornblende and garnet crystallization . . . 120
4.1.2. Small-scale REE variation in mafic rocks—Small eruptive centers (SEC) . . . 121
4.1.3. Extreme HREE depletion in the NSVZ . . . 123
4.1.4. Summary of along-strike and small-scale REE variations in the SVZ . . . 123
4.2. Variation of $^{87}Sr/^{86}Sr$ and $\delta^{18}O$ in the SVZ . . . 123
4.3. Variation of $^{143}Nd/^{144}Nd$ and $^{176}Hf/^{177}Hf$ in the SVZ . . . 124
4.4. Variation of Pb-isotope ratios in the SVZ . . . 126
4.5. U-series disequilibrium, $^{10}Be/^{9}Be$ and Th/La . . . 126
5. Synthesis of small- and large-scale trends . . . 128
5.1. Overview of magma generation in the TSVZ and CSVZ . . . 128
5.2. Geologic and geochemical reassessment of segments . . . 129
6. Conclusions . . . 129
Acknowledgments . . . 130
References . . . 130

1. Introduction

The Southern Volcanic Zone of the Andes (SVZ, Fig. 1 inset) is one of four segments of active convergent margin volcanism located on the west coast of South America, where the Cocos, Nazca, and Antarctic plates are subducted beneath the South American plate. Volcanic gaps between the segments are associated with convergence of thickened and buoyant oceanic lithosphere, resulting in a shallow subduction angle, and the pattern of volcanically active segments and intervening volcanic gaps along the Andes was early evidence of the importance of asthenospheric convection to produce mantle melting and arc magmatism (e.g., Thorpe, 1984). The thickness of the continental crust varies widely between the active segments, reaching Moho depths of 70 km beneath the Central Volcanic Zone (CVZ, Fig. 1 inset) compared with typical continental crustal thicknesses of 30 km beneath the Northern Volcanic Zone (NVZ), Austral Volcanic Zone (AVZ), and the southern part of the SVZ. The thick-crusted CVZ has been a primary location for investigating crustal processes affecting magmatism and continental crust building, including crustal assimilation, batholith formation, and crustal delamination (e.g., Mamani et al., 2010). The SVZ is important because features of the subducted Nazca plate vary along-strike, and depth to the Moho varies from about 55 to 30 km from north to south beneath the volcanic arc. This setting provides a natural laboratory for determining the relative contributions of slab, asthenosphere, mantle lithosphere, and crust to continental arc magmas.

Along-strike trends in volcanic rock characteristics in the SVZ have been studied since the early 1970s, resulting in a large body of work that delineates regional trends, as well as variations within individual volcanic centers. Distinct segments of the SVZ were proposed by Lopez-Escobar (1984) on the basis of petrologic characteristics of rocks and several different arrangements of segment boundaries have been proposed since then (Selles et al., 2004). Commonly four segments are identified (Fig. 1): the Northern Southern Volcanic Zone (33°–34.5°S NSVZ), the Transitional SVZ (34.5°S–37°S, TSVZ), the Central SVZ (37°S–41.5°S, CSVZ), and the Southern SVZ (41.5°S–46°SSVZ). Along-strike and cross-strike trends in geochemical characteristics of SVZ volcanoes were identified by Deruelle et al. (1983), Lopez-Escobar (1984), Hickey et al. (1984, 1986), Stern et al. (1984), Hildreth and Moorbath (1988), Morris et al. (1990), Sigmarsson et al. (1990), D. R. Tormey et al. (1991). These have been followed by numerous studies focused on specific volcanic complexes which greatly increase both the foundation of petrologic and geochemical data and the understanding of temporal and intra-volcano variability.

In this paper we 1) assess the evidence for proposed along-strike trends using an up-to-date database of high-quality geochemical analyses compiled from literature and original sources, 2) examine small-scale variations of the same parameters at one or more SVZ centers, and 3) use the contrasting spatial scales as a tool to determine sources of geochemical variation. Small-scale exceptions to large-scale trends are useful in identifying the sources of volcanism. Small-scale variations provide spatial limits on petrogenetic processes and help identify differing processes that produce the same geochemical results.

To examine along-strike trends, we use a database for volcanic rocks erupted at SVZ volcanoes compiled from published sources through 2015, including two supplementary data tables of previously unpublished major and trace element data, isotopic ratios of Sr, Nd, Pb, O, and U-series isotopic analyses.

2. Geologic background

2.1. Characteristics of the Nazca plate and Peru–Chile trench

The SVZ is bounded by Nazca plate features, the Juan Fernandez ridge in the north, and the Chile Rise in the south (Fig. 1). The Juan Fernandez ridge is an aseismic, volcanically inactive seamount chain and the Chile Rise is an active oceanic spreading center. Based on magnetic anomaly patterns, the age of the subducting oceanic lithosphere varies from about 35 Ma in the north to zero age at the Chile Rise (Tebbens et al., 1997). The Nazca plate has numerous fracture zones: the Mocha and Valdivia Fracture Zones displace seafloor that originated at the East Pacific Rise, and the Chiloe Fracture Zone and three successive offsets displace seafloor formed at the Chile Rise which is subducted at 47°S (Tebbens et al., 1997). Convergence is slightly oblique at about 80° and the convergence rate averages 7 cm/year (DeMets et al., 2010). The trench morphology changes from deep and sediment poor in the north to shallow and sediment filled toward the south (Voelker et al., 2013). Slab dip varies from 30 to 35° along the length of the SVZ with flattening just north of the NSVZ and at the southern extreme (Anderson et al., 2007; Hayes et al., 2012). The volcanic front occurs at 115–90 km above the Nazca plate surface (Tassara and Echaurren, 2012; Fig. 2).

2.2. Characteristics of the continental crust

The surface elevation of the base of SVZ frontal arc volcanoes varies from >3000 masl in the NSVZ to <1000 masl at 36–37°S and southward. Fig. 2 shows the depth to the sub-SVZ Moho, based on the gravity model of Tassara et al. (2006) and Tassara and Echaurren (2012). The crust thins from 55 km beneath the NSVZ to <35 km beneath the CSVZ and SSVZ, with the major zone of thinning beneath the TSVZ. Continental

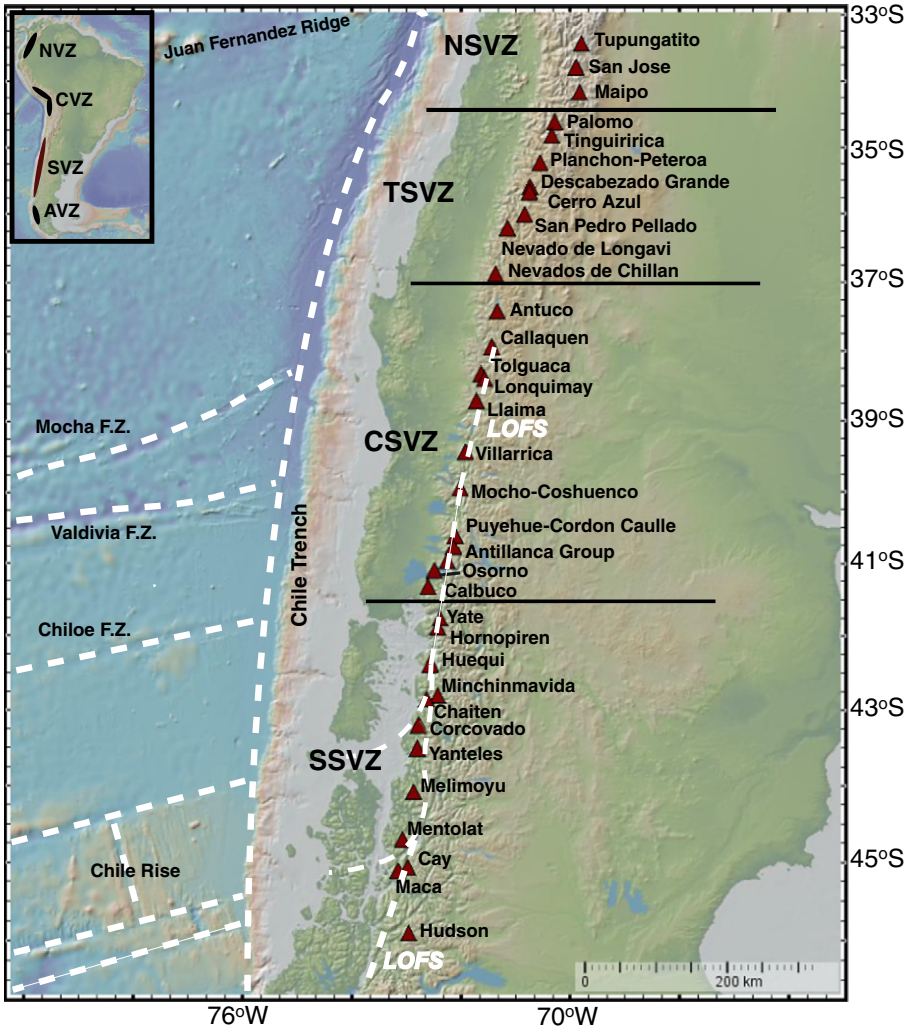

Fig. 1. Global multi-resolution topography (GMRT) synthesis map of the Southern Volcanic Zone (SVZ), showing volcanoes of the volcanic front (red triangles), Nazca Plate features and the Liquiñe–Ofqui Fault System (after Cembrano and Lara, 2009; Holbik, 2014). Segment boundaries (black lines) within the SVZ are Northern SVZ (NSVZ; 33–34.5°S), Transitional SVZ (TSVZ; 34.5–37°S), Central SVZ (CSVZ; 37–41.5°S), and Southern SVZ (SSVZ; 41.5–46°S), after Lopez-Escobar and Moreno, 1994. The Mocha, Valdivia, and Chiloe fracture zones and the Chile Rise on the Nazca plate, and the Liquiñe–Ofqui Fault System (LOFS; 38–47°S) are depicted by dashed white lines. The inset map shows the South American plate with the location of the four Andean volcanic zones. The map was constructed using GeoMapApp (http://www.geomapapp.org).

crustal lithologies vary beneath the volcanic front (Herve et al., 2007; Parada et al., 2007). Basement for the South American plate west of and beneath the SVZ consists of middle Paleozoic to Tertiary plutonic and metasedimentary rocks. The oldest rocks are in the coastal ranges and younger Mesozoic and Tertiary rocks dominate the orogenic belt. In the northern SVZ, volcanoes are on the continental divide and overlie late Paleozoic/Mesozoic plutonic and sedimentary rocks, intruded by Tertiary plutons. Similar rocks underlie parts of the TSVZ, although the arc front shifts to west of the continental divide. South of 37°S, plutons of the Mesozoic/Tertiary Patagonian batholith forms most of the volcanic front basement, together with low-grade metamorphic host rocks similar to those of the coastal Paleozoic accretionary complex exposed on the island of Chiloe and in archipelagos to the south (Herve et al., 2007). The tectonomagmatic history of the South American margin reveals that subduction magmatism, i.e., Paleozoic, Mesozoic, and Tertiary plutonic and volcanic rocks, has continued beneath the region of the SVZ region for about 300 Ma (Herve et al., 2007). The location of oldest rocks along the coast and evidence for an eastward shift in the location of the magmatic arc during the Tertiary has led to the conclusion that the continental margin in the northern SVZ has been significantly eroded by subduction (Kay et al., 2005; Stern et al., 2007; Stern, 2011). For example, Stern (2011) estimates rates of 115 km^3/km/Ma at 33–38°S and 35 km^3/km/Ma at 38–46°S over the last 30 Ma.

A long-recognized influence on the location of volcanic centers in the SVZ is the Liquiñe–Ofqui Fault System (LOFS) which extends 1200 km from 38°S to 47°S (Fig. 1). This is a transpressive, dextral strike-slip fault active over at least the last 6 Ma (Cembrano et al., 1996, 2000), as the result in part of oblique subduction of the Nazca plate. Cembrano and Lara (2009) examined the role of the fault system and related crustal stress state as a control on the location of volcanic edifices in the SVZ. They conclude that the existence of intra-arc fault systems is an important factor facilitating the ascent of magma through the crust in the SVZ. The N–S trending LOFS may serve as direct pathway for magmatic ascent in the CSVZ and SSVZ, and NE–SW tensional fractures related to the transpressional setting may be a second-order control on the location of volcanic centers.

Crustal xenoliths, ranging from single crystal xenocrysts to boulder-sized granitic bombs, are found at many SVZ volcanic centers. Studies of xenoliths at individual volcanoes have revealed both the nature of underlying crust and the nature of geochemical interactions between crust and magma at those volcanoes (Costa et al., 2002; Dungan, 2005; Hickey-Vargas et al., 1995; Lopez-Escobar and Moreno, 1981).

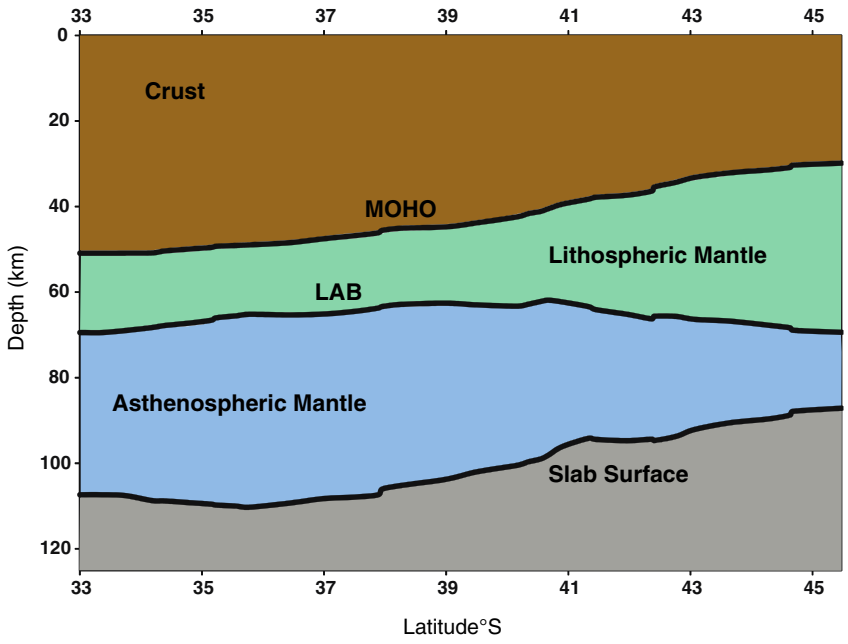

Fig. 2. Along-arc variation of depth to the Moho, lithosphere–asthenosphere boundary (LAB) and slab surface beneath arc front stratovolcanoes in the SVZ according to the 3-dimensional gravity model of Tassara et al. (2006) and Tassara and Echaurren (2012). Boundary lines are constructed using location points at the arc front volcanoes shown in Fig. 1, and ArcGIS contour extrapolation. An exponential smoothing equation is applied. The errors in the boundary locations inherent in the Tassara et al. (2006) model are MOHO = 5 km, LAB = 10 km, slab surface = 25 km.

2.3. Inferences about the mantle wedge

Fig. 2 shows the position of Moho, lithosphere–asthenosphere boundary (LAB), and slab surface beneath SVZ volcanic front volcanoes based on the gravity model of Tassara et al. (2006) and Tassara and Echaurren (2012). Although the slab flattens to the north of the NSVZ, shallowing of the slab occurs northward of SVZ volcanoes. The volcanic front lies further from the trench in the NSVZ and overlies the slab at a depth of 115 km, which diminishes to 100–85 km through most of the SVZ until the Chile Rise is approached. The Tassara et al. (2006) model infers a relatively uniform depth for the regional LAB at 60–70 km, thus the mantle lithosphere thins where crust thickens. In a cross-arc seismic study at the latitude of Villarrica Volcano (39.4°S), Dzierma et al. (2012a, 2012b) and Thorwart et al. (2014) find slab dip of about 35° and crustal thicknesses of 30–40 km, thickening toward the east. They also find a velocity maximum at about 50 km in the back arc, possibly marking the lithosphere–asthenosphere boundary. Velocities are lower beneath the arc than beneath the forearc, consistent with melt or fluid beneath the volcanic front (Thorwart et al., 2014) and a possible shallowing of the local lithosphere–asthenosphere boundary.

3. Geochemical and petrologic background

3.1. Review of geochemical and petrologic studies delineating along-strike trends

3.1.1. Segments of the SVZ

Primary studies of SVZ volcanic centers by Chilean geologists defined along-strike differences in the character of their eruptive products (Lopez-Escobar, 1984). Basaltic products (basalts and basaltic andesites) are dominant in the late Pleistocene–recent stratovolcanoes from Antuco volcano at 37.4°S southward to Osorno volcano at 41°S. North of Antuco in the TSVZ, basalts are rare, and volcanic products are varied and include andesite, dacite, and rhyolite. At the northernmost volcanic centers, such as San Jose and Maipo in the NSVZ, hornblende-bearing andesite is abundant. Based on these petrological changes, Lopez-Escobar (1984) divided the SVZ into two segments: Province I (33–37°S), and Province II (37–46°S). Three segments were proposed by Tormey et al. (1991a) based on bulk rock major element composition: the Northern SVZ (33–34.5°S); Transitional SVZ (34.5°S–37°S), and Southern SVZ (south of 37°S). The SSVZ was later subdivided into the Central SVZ and Southern SVZ (south of 41.5°S) by Lopez-Escobar and Moreno (1994), although volcanoes to the south were sparsely studied (Lopez-Escobar et al., 1993). As the database has grown, several iterations of the segments have been made (Selles et al., 2004).

3.1.2. Along-strike geochemical variations

Several geochemical trends accompany these petrologic observations.

1) Among basaltic to intermediate rocks (basalts, basaltic andesites, and andesites), ratios of LREE (light rare earth elements) to HREE (heavy REE) increase northward, reaching extreme values, La/Yb up to 28, in some northernmost volcanic centers (Hickey et al., 1986; Hildreth and Moorbath, 1988; Lopez-Escobar, 1984; Stern et al., 1984; Tormey et al., 1991a). This trend, particularly the low HREE contents at NSVZ volcanoes was attributed to either garnet in the thick crust or to a decreasing extent of partial melting of garnet lherzolite in the mantle (Tormey et al., 1991a). A third process, subduction erosion of the forearc crust and melting along the slab-mantle boundary, was also proposed (Stern et al., 1984). In a summary of SVZ magmatism, López-Escobar et al. (1995a) divided all SVZ basaltic rocks into two types—Type 1, having the low LREE/HREE common in largely basaltic CSVZ volcanoes, and Type 2, having higher LREE/HREE, as found in back arc volcanoes, such as Laguna del Maule and Lanin, most NSVZ and TSVZ centers, and numerous small eruptive centers found along the LOFS in the CSVZ.
2) Low $^{143}Nd/^{144}Nd$, high $^{87}Sr/^{86}Sr$, and $\delta^{18}O$ is coupled with high LREE/HREE in the NSVZ andesitic volcanoes (Hickey et al., 1986; Hildreth and Moorbath, 1988). Lower $^{87}Sr/^{86}Sr$ ratios and higher $^{143}Nd/^{144}Nd$ ratios, together with mantle-like $\delta^{18}O$ are observed in volcanoes of the CSVZ (Deruelle et al., 1983; Hickey et al., 1986; Hildreth and Moorbath, 1988). Osorno and Calbuco volcanoes at 41.1°S and 41.3°S in the CSVZ were found to reverse this trend with higher

$^{87}Sr/^{86}Sr$ and $\delta^{18}O$, and lower $^{143}Nd/^{144}Nd$ (Deruelle et al., 1983; Hickey et al., 1986). Hildreth and Moorbath (1988) attributed these changes, like higher LREE/HREE, to crustal interaction in the NSVZ and TSVZ, with isotope ratios reflecting either greater assimilation of crust compared with volcanoes to the south, due to its enhanced thickness, or assimilation of crust with a more sedimentary or older character. These findings led to the concept of deep crust/Moho focused MASH zones (melting, assimilation, storage, and homogenization) controlling the baseline geochemical character of mafic magmas erupted at volcanoes along the SVZ arc (Hildreth and Moorbath, 1988).

Unlike LREE/HREE ratios and Sr and Nd isotopes, Pb-isotopes showed no systematic along-strike variation in the segments of the SVZ. On plots of $^{207}Pb/^{204}Pb$ and $^{208}Pb/^{204}Pb$ versus $^{206}Pb/^{204}Pb$, SVZ rocks plot within the field for Nazca plate sediments (Dasch, 1981). Hickey et al. (1986) argued that Pb extracted from subducted sediment dominated the Pb-isotopic composition of the SVZ lavas, in comparison to mantle wedge sources. Hildreth and Moorbath (1988) maintained that the Pb-isotopic composition of the average SVZ upper crust, represented by river mouth sediments, overlapped with the active volcanic arc, such that subducted sediment and crustal sources could not be distinguished.

3) U-series isotopic disequilibrium (excess ^{238}U relative to ^{230}Th), ^{10}Be activity ($^{10}Be/^{9}Be$) and B enrichment (high B/Be) were proposed and tested as unequivocal indications that subducted sediment or slab-derived fluids were added to the mantle sources of SVZ arc magmas (Morris et al., 1990; Sigmarsson et al., 1990, 2002). ^{10}Be and ^{230}Th are time-sensitive radioactive tracers, with half-lives 1.5×10^6 y and 7.5×10^4 y, respectively. ^{10}Be in an arc rock records the incorporation of Be from young subducted sediment, whereas excess or deficient ^{230}Th compared with parent ^{238}U records the fractionation of fluid mobile U from fluid-immobile Th during dehydration of the subducted slab or subsequent melting processes. B is exceptionally fluid mobile, like U, and records the incorporation of slab-derived fluids in the sources of arc magmas. Morris et al. (1990) found a marked correlation of the trace element ratio B/Be and $^{10}Be/^{9}Be$ in arcs worldwide. Limited $^{10}Be/^{9}Be$ data for the SVZ showed a maximum of $4–6 \times 10^{-11}$ in basalts from volcanoes Villarrica and Osorno, and small but detectible amounts in basalts from other SVZ volcanoes. Worldwide, these correlations were interpreted to indicate varying amounts of young sediment and fluid added to a mantle source. In the case of the SVZ, however, the possibility that dilution of the subduction signal by ^{10}Be-free ancient crustal assimilants was also considered (Morris et al., 1990).

Several SVZ centers were found to exhibit excess ^{238}U (Sigmarsson et al., 1990, 2002). Similar to $^{10}Be/^{9}Be$ results, highest ($^{238}U/^{230}Th$) was found in CSVZ basaltic volcanoes, especially Villarrica, and Osorno, whereas rocks from other CSVZ volcanoes, Mocho and Antuco, TSVZ volcano Nevados de Chillan, and San Jose (NSVZ) approach secular equilibrium. A narrow range of ($^{230}Th/^{232}Th$) ratios was noted for the SVZ (0.8–0.9), with Osorno as an outlier with ($^{230}Th/^{232}Th$) of about 0.7.

3.2. Re-examination of trends

Recent research has greatly enriched the size and quality of the database for SVZ volcanic centers. Focused studies on volcanic centers Villarrica, Puyehue, Planchon–Peteroa, Tatara–San Pedro, Quizapu, and Llaima (Costa and Singer, 2002; Davidson et al., 1987, 1988; Dungan et al., 2001; Feeley and Dungan, 1996; Feeley et al., 1998; Ferguson et al., 1992; Gerlach et al., 1988; Hickey-Vargas et al., 1989; Hildreth and Drake, 1992; Holbik, 2014; Jicha et al., 2007; Lara et al., 2006a; Reubi et al., 2011; Ruprecht et al., 2012; Ruprecht and Cooper, 2012; Singer et al., 1997, 2008; Tormey et al., 1995; Schindlbeck et al., 2014), provide insights into magma differentiation processes and connections between magma geochemistry, crustal assimilation, and eruptive cycles. Such studies are essential to distinguish geochemical trends caused by local versus regional processes. New studies of volcanoes Huequi, Cay, Maca, and Hudson (D'Orazio et al., 2003; Gutierrez et al., 2005; Naranjo and Stern, 1998; Stern and Naranjo, 2015; Watt et al., 2011a, 2011b) extend coverage to the SSVZ. In addition, recent regional studies interpret along-strike, across-strike, and other regional geochemical variations (Holbik, 2014; Holm et al., 2014; Jacques et al., 2013, 2014; Watt et al., 2013; Wehrmann et al., 2014). Studies by Jacques et al. (2013, 2014) and Holbik (2014) add Hf-isotope data.

3.2.1. Definition of petrologic character

In order to distinguish variations resulting from along-strike changes in magma generation processes from post-melting magma differentiation processes, we show along-strike geochemical parameters coded for rock type. It is well-recognized that mantle-derived primary basalts are not present in the SVZ. True basalts (<52% SiO_2) are rare (Figs. 3 and 4), although many volcanic centers are characterized as basaltic. In order to interpret mantle-related geochemical trends that can be overprinted by crustal processes, researchers select primitive basalt compositions either 1) by choosing most mafic whole-rock compositions at a particular volcanic center based on SiO_2, MgO, or Mg# or 2) by projecting inferred crystallization trends from intermediate toward mafic compositions (e.g., Plank and Langmuir, 1988). In the SVZ, the former method is complicated by the occurrence of cumulate or xenocrystal olivine and plagioclase (Fig. 3); the latter is complex because evolved magmas are frequently mixed and/or saturated with multiple phases in proportions that change with depth (e.g., Grove and Baker, 1984). For this work, we use a classification of volcanic rocks based on SiO_2 content (Fig. 3). Basaltic rocks are defined as basalt (<52% SiO_2) and basaltic andesite (52–56% SiO_2). Although the focus of this work is on basaltic rocks, we explore variations in intermediate and silicic rocks when they provide information relevant to other trends.

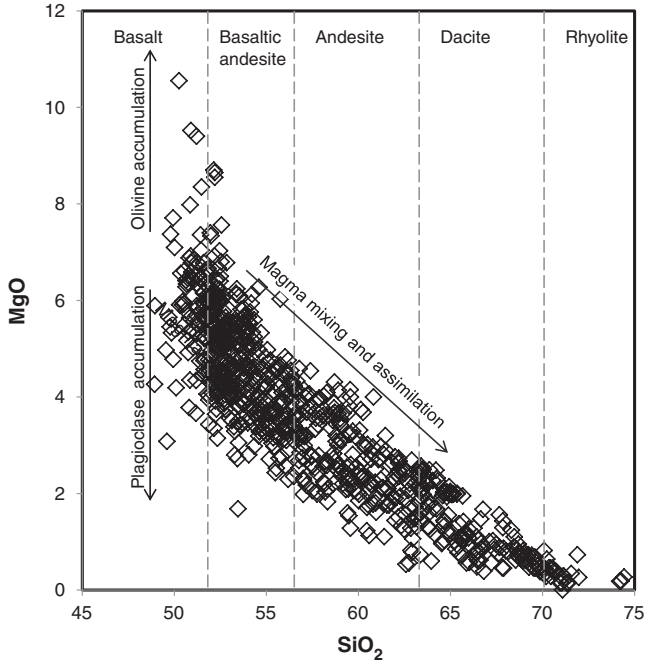

Fig. 3. Plot of MgO versus SiO_2 for volcanic rocks discussed, showing the distribution of published rock compositions. Data are from Supplementary Table 1 and Davidson et al. (1987, 1988), D'Orazio et al. (2003), Ferguson et al. (1992), Fierstein et al. (1989), Futa and Stern (1988), Gerlach et al. (1988), Gutierrez et al. (2005), Hickey et al. (1986), Hickey-Vargas et al. (1989), Hildreth and Moorbath (1988), Holm et al. (2014), Jacques et al. (2013, 2014), Jicha et al. (2007), Lopez-Escobar et al. (1993, 1995b), McMillan et al. (1989), Reubi et al. (2011), Ruprecht et al. (2012), Schindlbeck et al. (2014), Selles et al. (2004), Singer et al. (2008), Sruoga et al. (2005, 2012), Tormey et al. (1995), Watt et al. (2011a), Wehrmann et al. (2014).

Similarly, we focus on rocks from SVZ stratovolcanoes of the volcanic front, but we also explore some trends in volcanoes which are behind the arc front, and small eruptive centers.

3.2.2. Large-scale along-strike variations

Figs. 4 through 11 summarize the variation of geochemical parameters along-strike of the SVZ, including data published through 2015. In the following sections, we discuss whether trends discussed in Section 3.1 are confirmed by new data, the origin of exceptions to trends, and new observations that may help in understanding the processes that created along-strike geochemical trends in the SVZ.

4. Discussion

4.1. Along-strike variation of SiO_2 and REE

The along-strike variation of petrologic character in the SVZ defined by early researchers remains valid. Many volcanic front volcanoes from the TSVZ/CSVZ boundary southward have basalts and basaltic andesites, whereas basalts are entirely absent from the NSVZ. The northernmost volcano having true basalt is Planchon–Peteroa. Variation from basalt through dacite is common at volcanic front volcanoes south of the TSVZ, without geographic pattern, while rhyolite is rare. A few volcanoes in the TSVZ, CSVZ, and SSVZ, e.g., Mocho, Calbuco, Huequi, are composed entirely of intermediate rocks, similar to those of the NSVZ.

Overall, LREE/HREE ratios decrease along-strike from the NSVZ through the CSVZ, starting from high values of La/Yb = 11–28 in hornblende-bearing andesites from the NSVZ (Lopez-Escobar, 1984). Along the TSVZ–CSVZ transect, minimum La/Yb ratios in basaltic rocks decrease from >5 to <5 between Callaquen (>5) and Tolguaca (<5), and La/Yb ratios are less variable at CSVZ volcanoes. The low La/Yb ratios <5 characteristic of basalts and basaltic andesites in the CSVZ are also found at many SSVZ volcanoes, except for Hudson volcano and Corcovado (43.2°S). Notable exceptions to these trends are basaltic andesites and andesites of Nevado de Longaví (TSVZ), Calbuco (CSVZ), and Huequi (SSVZ) volcanoes, which display large intra-volcano variations compared with adjacent volcanoes (Figs. 5 and 12), and basalts from mafic small eruptive centers sited along the Liquiñe–Ofqui Fault System, which commonly, but not always, have La/Yb > 5 (López-Escobar et al., 1995a; Fig. 13).

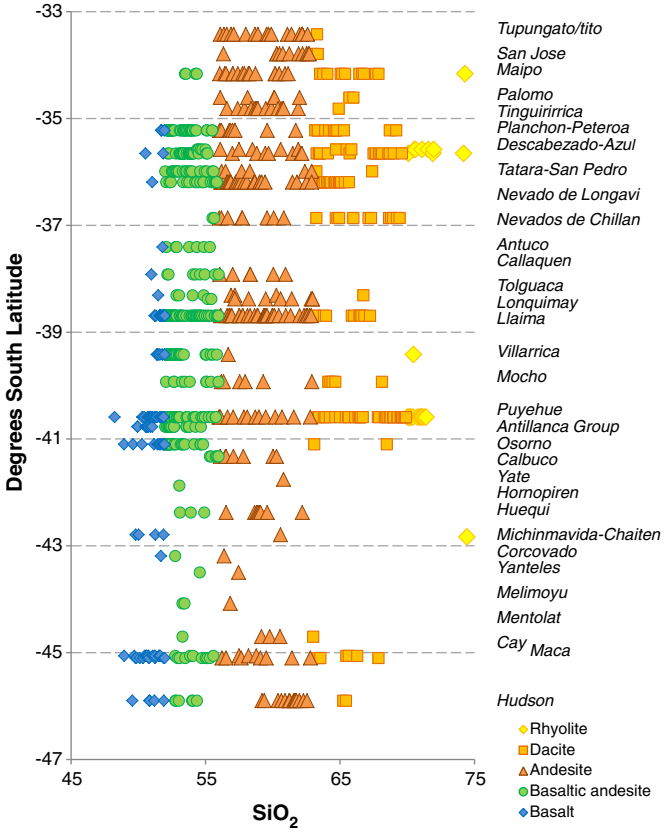

Fig. 4. Plot of SiO_2 versus latitude for rocks from SVZ volcanic front volcanoes. Data are from sources listed in Fig. 3.

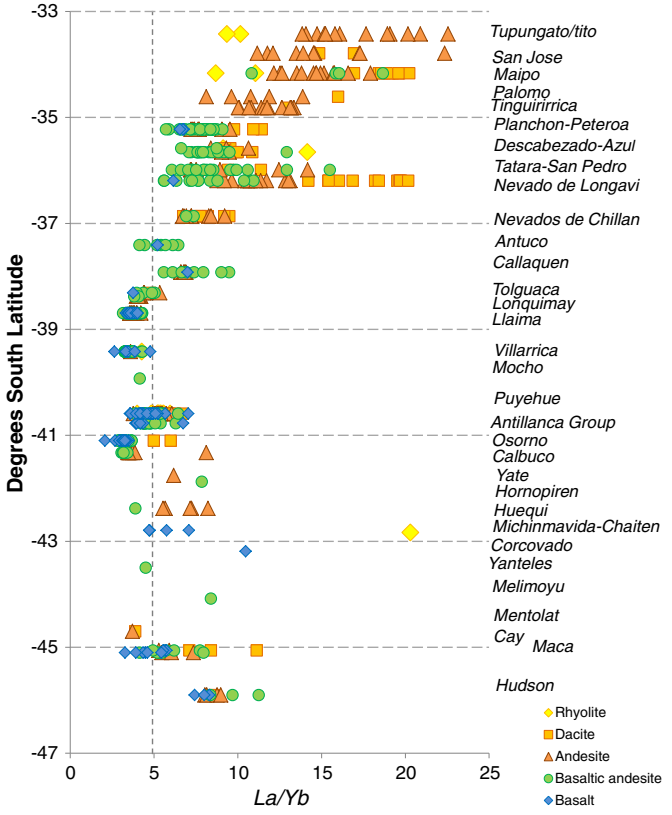

Fig. 5. Plot of La/Yb versus latitude for rocks from from SVZ volcanic front volcanoes. Data are from sources listed in Fig. 3. Note that NSVZ volcano Tupungato/tito has andesite and dacite with La/Yb = 25–28.

4.1.1. The role of hornblende and garnet crystallization

Selles et al. (2004) and Rodriguez et al. (2007) interpreted the large range of LREE/HREE in Nevado de Longavi dacites and associated basaltic andesitic inclusions as the result of hornblende fractionation, with possible minor garnet fractionation during deep crustal processing. Both garnet and amphibole have mineral/melt partition coefficients >1 for HREE; consequently, fractionation of either mineral limits increase in HREE and causes increasing LREE/HREE. MREE are also compatible in hornblende, resulting in low MREE/HREE ratios in the coexisting melt (e.g., Dy/Yb, Davidson et al., 2007). Unlike the majority of TSVZ and CSVZ volcanoes where hydrous minerals are limited to dacitic and rhyolitic compositions, if they appear at all, hornblende is a phenocryst in basaltic andesitic inclusions at Nevado de Longavi. Andesites from Huequi are also hornblende-bearing (Watt et al., 2011a) and andesites from Calbuco contain pseudomorphic clots of fine hornblende breakdown products, including pyroxene, plagioclase and abundant oxides, and cognate hornblende-bearing gabbroic inclusions (Hickey-Vargas et al., 1995; Lopez-Escobar et al., 1995b). Fig. 12 shows the significant differences in REE patterns of lavas affected by amphibole fractionation compared to an amphibole-free suite (e.g., Puyehue). In SVZ volcanic suites, hornblende fractionation results in lower abundances of highly incompatible elements, such as K, Ba, and La relative to SiO_2, compared with those produced by fractionation of

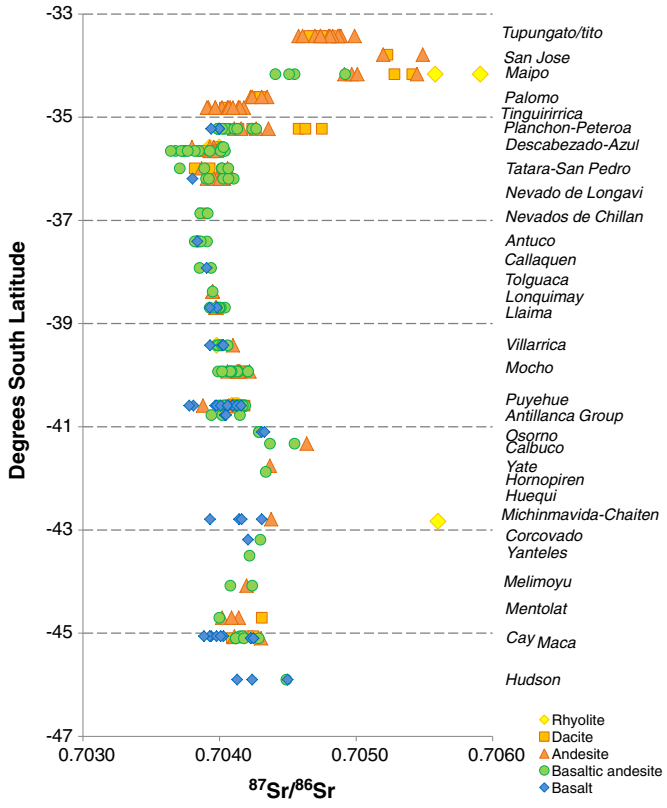

Fig. 6. Plot of $^{87}Sr/^{86}Sr$ versus latitude for rocks from SVZ volcanic front volcanoes. Data are from Supplementary Table 2 and Davidson et al. (1987, 1988), D'Orazio et al. (2003), Deruelle et al. (1983), Futa and Stern (1988), Gerlach et al. (1988), Harmon and Hoefs (1984), Hickey et al. (1986), Hickey-Vargas et al. (1989), Hildreth and Moorbath (1988), Holm et al. (2014), Jacques et al. (2013, 2014), Lopez-Escobar et al. (1993, 1995b), McMillan et al. (1989), Reubi et al. (2011), Rodriguez et al. (2007), Selles et al. (2004), Singer et al. (2008), Stern et al. (1984), Tormey et al. (1995), Wehrmann et al. (2014).

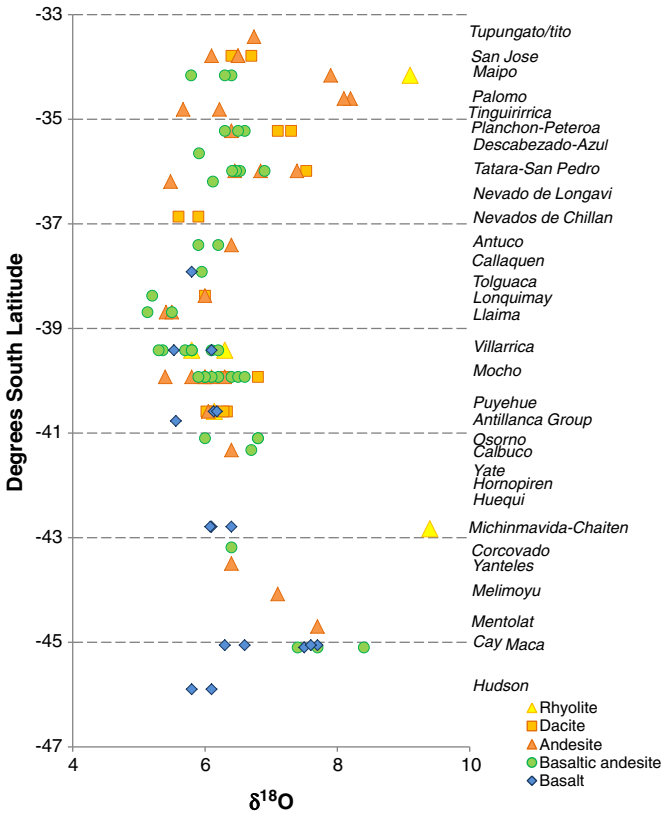

Fig. 7. Plot of $\delta^{18}O$ versus latitude for rocks from SVZ volcanic front volcanoes. Data are from sources listed in Fig. 6.

anhydrous mineral assemblages (Fig. 12c). SiO_2 increases more rapidly with SiO_2 poor hornblende-bearing assemblages, resulting in an apparent depression of incompatible element abundances in intermediate rocks (Lopez-Escobar et al., 1995b; Rodriguez et al., 2007). HREE contents are constant or decrease slightly in these rocks, LREE increase and LREE/HREE rise over a limited range of SiO_2.

Important questions are 1) why does hornblende occur in mafic magmas only at Nevado de Longavi, Calbuco, and Huequi; and 2) can the HREE depletion as reflected by the high La/Yb in some lavas, e.g., andesites from Nevados de Longavi and one sample from Calbuco, be attributed to garnet crystallization (Fig. 12b). Experimental studies of arc magma compositions at pressures of 1.2 GPa, comparable to lower crustal depths in the TSVZ and sub-Moho depths in the CSVZ, show that garnet is a liquidus phase in basaltic magma at high water contents >6%, joined by amphibole at <1070 °C (Müntener et al., 2001). Assemblages with mineral chemistry similar to these experimental products are in exposed deep arc sections, such as Talkeetna and Kohistan (Müntener et al., 2001). In andesitic magma, garnet and clinopyroxene are liquidus phases in H_2O-rich compositions at pressures of 0.8–1.2 GPa and temperatures >950 °C, whereas lower temperatures and/or higher water contents stabilize amphibole (Alonso-Perez et al., 2009). Since basalts are not present at these volcanoes, an alternative explanation for HREE depletion could be that basaltic magmas, similar to those from adjacent volcanoes, assimilated low HREE partial melts of aluminous, garnet-bearing crustal rocks. Rocks from Calbuco are convincingly contaminated, having lower $^{143}Nd/^{144}Nd$ and higher $^{87}Sr/^{86}Sr$ than surrounding volcanoes, and Lopez-Escobar et al. (1995b) proposed that the excess water needed to stabilize hornblende in the parental magma was derived from assimilated mica- and amphibole-bearing schists, similar to those that outcrop just south of the volcano. In contrast, neither Nevado de Longaví nor Huequi have geochemical markers of crustal contamination, or correlations between HREE depletion and isotopic composition. Selles et al. (2004) and Rodriguez et al. (2007) proposed instead that the high water content at Nevado de Longaví was a feature of primary mantle-derived magma, possibly correlated with the location of the volcano over the subducted extension of the Nazca Plate Mocha fracture zone. Dewatering of serpentine in the hydrated mantle lithosphere of subducting plates has been proposed as a source for fluids causing melting in the overlying asthenosphere, and enhanced dewatering related to fracture zones has been hypothesized in other locations (Jicha et al., 2004; Singer et al., 1996). A similar relationship has been suggested for Calbuco and the Chiloe fracture zone (Fig. 1), but Nazca plate fracture zones do not exactly match the distribution of hornblende-bearing rocks in the SVZ. Volcanoes Yate and Michinmahuida, which have anhydrous assemblages, are found between Calbuco and Huequi, for example, and hornblende-bearing rocks are not associated with the Valdivia fracture zone. The cause of hornblende saturation at volcanoes in the TSVZ, CSVZ, and SSVZ remains a puzzle, although it generally does not appear to be related directly to either assimilation of crustal rocks or crustal thickness.

4.1.2. Small-scale REE variation in mafic rocks—Small eruptive centers (SEC)

López-Escobar et al. (1995a) noted that most basalts from small monogenetic scoria cones found along the Liquiñe–Ofqui Fault System throughout the CSVZ have high LREE/HREE similar to CSVZ basaltic lavas from behind the volcanic front and the TSVZ. López-Escobar et al. (1995a) referred to these basalts as Type 2, quite different from Type 1 basalts with La/Yb <5 that are typical of CSVZ stratovolcanoes. Notable clusters of SEC are those near Villarrica Volcano (Hickey-Vargas et al., 1989, 2002); the Carran-Los Venados volcanic

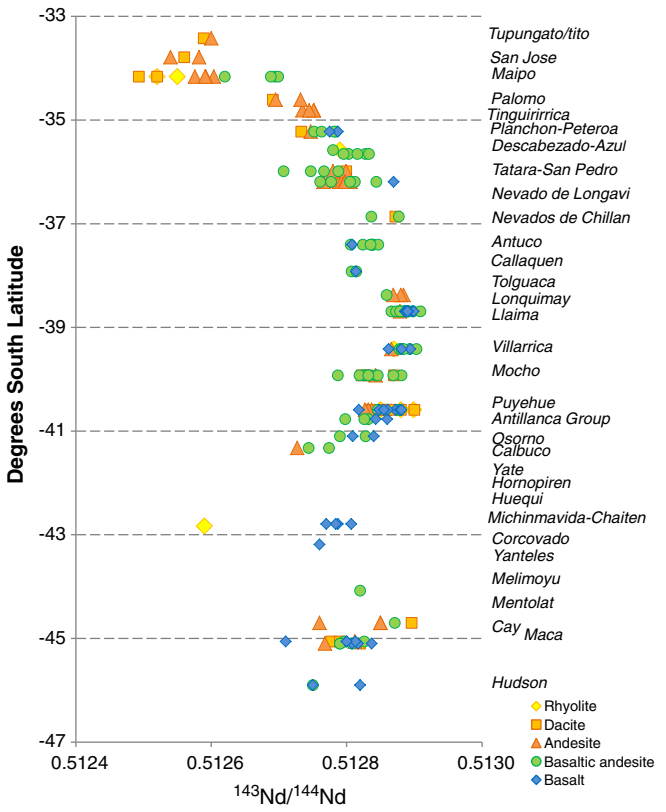

Fig. 8. Plot of $^{143}Nd/^{144}Nd$ versus latitude for rocks from SVZ volcanic front volcanoes. Data are from sources listed in Fig. 6.

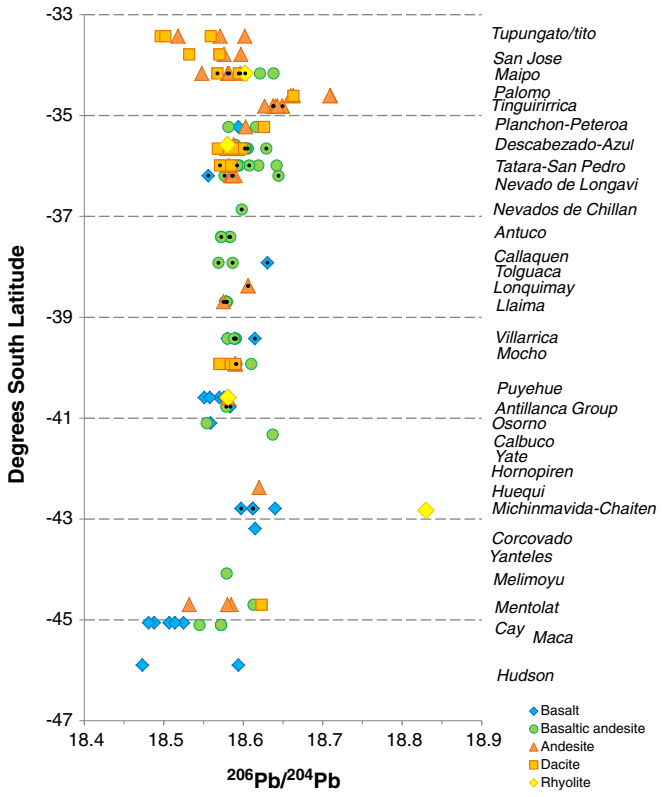

Fig. 10. Plot of $^{206}Pb/^{204}Pb$ versus latitude for rocks from SVZ volcanic front volcanoes. Data are from sources listed in Fig. 6. Small black dots are high precision Pb-isotope data from Jacques et al. (2013, 2014) and Holm et al. (2014).

field north of Puyehue (Lara et al., 2006b; Rodríguez, 1999); Cordon Cenizos, northeast of Osorno Volcano, and scattered centers east of Calbuco Volcano (Lopez-Escobar et al., 1995b). Although most SEC basalts are more LREE enriched than nearby stratovolcano basalts, each SEC field, and in some cases each scoria cone, has distinct geochemical characteristics.

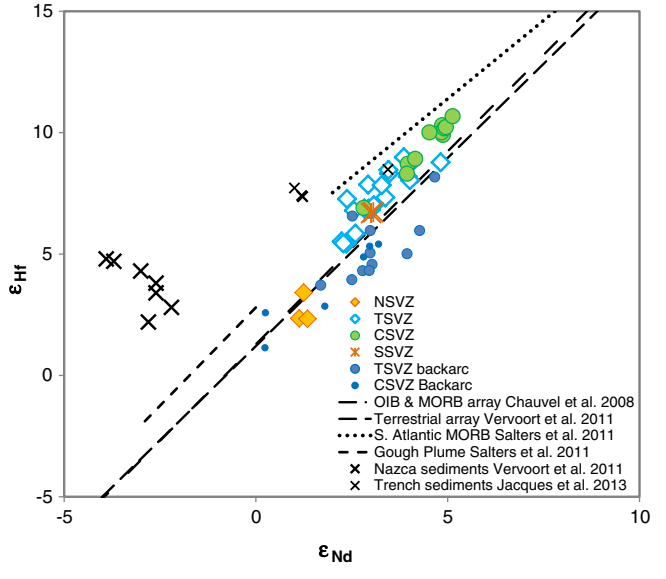

Fig. 9. Plot of ε_{Hf} versus ε_{Nd} showing data for basaltic rocks from SVZ segments. Data are from Jacques et al. (2013, 2014) and Holbik (2014). Basaltic rocks from the Andean back arc in Argentina are shown by blue filled circles (Jacques et al., 2013, 2014). Nazca plate sediments (Vervoort et al., 2011) and Chile trench sediments (Jacques et al., 2013) are shown by large and small X symbols, respectively. The terrestrial array of Vervoort et al. (2011), the MORB-OIB array of Chauvel et al. (2008) and correlation lines for South Atlantic MORB and the Gough mantle plume (South Atlantic) from Salters et al. (2011) are shown for comparison.

In the Villarrica region SEC are distributed over an area of about 20 km^2 to the north and east of Villarrica stratovolcano, with a clear relationship to the LOFS (Cembrano and Lara, 2009). Although most SEC erupted Type 2 basalts (La/Yb = 6–11; Fig. 13), one SEC is composed of basaltic scoria and lava flows identical in character to Villarrica Volcano basalts (Type 1; La/Yb < 5; Fig. 13) (Hickey-Vargas et al., 2002, 2016). Since these basalts are among the most mafic in the SVZ, with Fo 90 olivine phenocrysts, SiO_2 < 52%, MgO = 6–10% in non-accumulative samples, and Mg# 58–68 (Hickey-Vargas et al., 2016), the origin of the REE variation is likely related to mantle processes rather than differentiation or crustal assimilation processes. Model calculations for REE during melting of peridotite indicate that the array of REE abundances and La/Yb ratios found in Type 1 and Type 2 primary magmas for the SEC cannot be produced by varying the extent of melting of a single source, i.e., a source with homogeneous trace element composition and the same modal mineralogy (Fig. 13). Because Yb contents are similar in basalts with differing La/Yb, sources must have significantly different La/Yb or different residual mineral assemblages. For the latter case, modes of 30–40% clinopyroxene are required to match HREE concentrations and La/Yb ratios (Fig. 13). In these SEC lavas, Sr, Nd, and Hf-isotope, ($^{238}U/^{230}Th$) and $^{10}Be/^{9}Be$ ratios are correlated with La/Yb (Hickey-Vargas et al., 2002, 2016). Based on these geochemical parameters and the spatial distribution of the SEC, Hickey-Vargas et al. (2002, 2016) proposed that the less LREE-enriched SEC and stratovolcano basalts formed from the ambient (Type 1) sub-CSVZ asthenospheric mantle, whereas more LREE-enriched, Type 2 SEC included partial melts of pyroxenite in the sub-CSVZ mantle lithosphere. Evidence for the pyroxenite melts was enhanced by the small magma volume of the fault-related SEC.

As shown in Fig. 13, REE characteristics among the Villarrica region SEC closely parallel REE differences between basaltic rocks from the

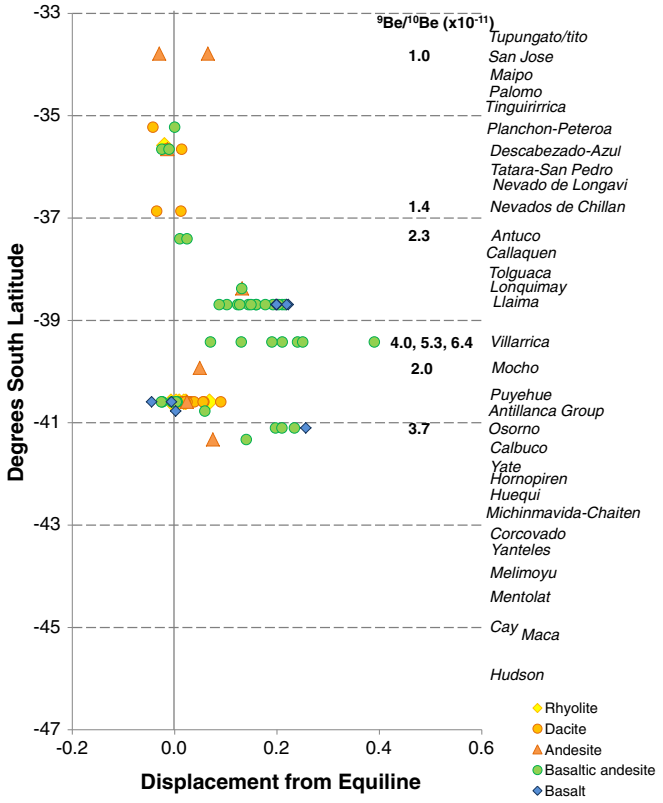

Fig. 11. Plot of ^{238}U excess (see text for explanation) and $^{10}Be/^{9}Be$ ($\times 10^{-11}$) versus latitude for rocks from SVZ volcanic front volcanoes. Data are from Supplementary Table 2 and Hickey-Vargas et al. (2002), Jicha et al. (2007), Morris et al. (1990), Reubi et al. (2011), Ruprecht and Cooper (2012), Sigmarsson et al. (1990, 2002), Tormey et al. (1991b).

TSVZ and CSVZ. Differences in REE characteristics between the TSVZ and CSVZ have been attributed to a wide variety of processes. Hildreth and Moorbath (1988) attributed higher LREE/HREE to interaction with garnet-bearing lower crust, as part of the lower crustal MASH zone model. Tormey et al. (1991a) proposed that mantle beneath the TSVZ melted to a smaller extent, as the result of a smaller melting column between subducted slab and thickened lithosphere, thus restricting asthenospheric circulation, when compared with the CSVZ. More recently, Jacques et al. (2013, 2014) proposed that the extent of mantle partial melting diminished in the TSVZ as the result of a smaller input from slab-derived fluids, and then used the Arc Basalt Simulator (ABS Version 3; Kimura et al., 2009), to quantitatively model geochemical differences between mafic magmas from volcanoes in the TSVZ and CSVZ. Their best fit results were consistent with a smaller contribution of slab-derived fluids in the TSVZ compared with the CSVZ, a larger proportion of sediment compared with altered oceanic crust (AOC) in the TSVZ, and a lower extent of melting of the asthenosphere. Similar models related to progressive slab dehydration with depth have been proposed to explain geochemical differences between magmas of the volcanic front and behind the front or back arc volcanoes (Hickey-Vargas et al., 1989; Jacques et al., 2013; Lara et al., 2004; López-Escobar et al., 1995a; Stern et al., 1990; Watt et al., 2013).

4.1.3. Extreme HREE depletion in the NSVZ

With exceptions noted above, andesites from the NSVZ have systematically higher LREE/HREE than those from other parts of the SVZ, and some are notably depleted in HREE, with abundances of <5 X chondrites (Fig. 12d; Lopez-Escobar, 1984). The correlation between the occurrence of HREE depletion in volcanic rocks of the NSVZ, the thick crust that results in pressures within the stability field of garnet and the compatibility of HREE in garnet, has led to the proposition that low HREE contents and high LREE/HREE are caused by contamination of ascending magma by assimilation of thick lower continental crust (Hildreth and Moorbath, 1988). Similarly, HREE depletion and high LREE/HREE ratios in ancient volcanic rocks have been used as a proxy for crustal thickening in the interpretation of temporal trends in the Andes and elsewhere (e.g., Kay et al., 2005). In the NSVZ, volcanic rocks are also characterized by much higher $^{87}Sr/^{86}Sr$ and lower $^{143}Nd/^{144}Nd$ (Figs. 6 and 8) than the rest of the SVZ, which supports their incorporation of additional or older crustal material compared with the TSVZ, CSVZ, and SSVZ. An alternative interpretation for these isotopic characteristics is that crustal material was incorporated through subduction erosion; that is, crust is removed from the continental margin, subducted, and then recycled into the zone of arc magma generation (Holm et al., 2014; Kay et al., 2005; Stern et al., 1984). This hypothesis is supported by the geologic evidence for removal of large amounts of crust from the upper plate since the Pliocene (Kay et al., 2005; Stern et al., 2007; Stern, 2011). In models involving either assimilation of lower crust or subducted continental crust, high La/Yb can be imparted as the result of residual garnet stabilized at high pressure; therefore, REE character is not useful in distinguishing these hypotheses unless it is correlated with other geochemical markers of crustal assimilation or subduction inputs. For example, for Maipo volcano, Holm et al. (2014) support the subduction erosion model, based on isotopic modeling which is consistent with addition of subducted upper continental crust to magma sources. In contrast, Sruoga et al. (2012) support in situ crustal assimilation for Maipo based on isotopic evidence, in addition to marked textural disequilibrium between melt and minerals.

4.1.4. Summary of along-strike and small-scale REE variations in the SVZ

Based on our comparisons, at least four distinct causes for variations in La/Yb ratios and normalized REE patterns can be identified in mafic SVZ magmas:

1) crystallization of hornblende and possibly garnet from mafic magma, possibly connected to unusually high primary water contents (Lopez-Escobar et al., 1995b; Rodriguez et al., 2007; Selles et al., 2004; Sruoga et al., 2012; Watt et al., 2011a);
2) incorporation of partial melts of garnet-bearing or garnet-free pyroxenite, in the lower crust (Ferguson et al., 1992; Hildreth and Moorbath, 1988; Tormey et al., 1995) and/or mantle lithosphere (Hickey-Vargas et al., 2002, 2016);
3) along-strike changes in the extent of partial melting of mantle asthenosphere (Jacques et al., 2014; Tormey et al., 1991a), possibly related to differing contributions of slab-derived fluids (Jacques et al., 2014), or to thickening of the lithosphere and decreased circulation in the asthenosphere (Tormey et al., 1991a); and
4) partial melting of material eroded by subduction from the continental crust, with subsequent mixing with asthenospheric melts (Stern et al., 2007; Stern, 2011; Holm et al., 2014).

4.2. Variation of $^{87}Sr/^{86}Sr$ and $\delta^{18}O$ in the SVZ

As shown in Fig. 6, $^{87}Sr/^{86}Sr$ ratios in the SVZ decrease from high values of 0.7056 in andesites and dacites from NSVZ volcanoes Maipo and San Jose, to values as low as 0.7037 in mafic lavas from TSVZ volcanoes Cerro Azul and Tatara–San Pedro. $^{87}Sr/^{86}Sr$ ratios in basaltic rocks rise slightly through the CSVZ and then rise abruptly to >0.7042 at Volcan Osorno. Ratios of $^{87}Sr/^{86}Sr$ vary within the SSVZ, but overall they are similar to those of the CSVZ and TSVZ lavas.

Increasing $^{87}Sr/^{86}Sr$ with increasing SiO_2 in rocks from an individual volcanic center is strong evidence for assimilation of radiogenic sialic upper crustal rocks during differentiation. In the TSVZ, elevated $^{87}Sr/^{86}Sr$ ratios in some but not all dacitic to rhyolitic rocks are observed at volcanic complexes Planchon–Peteroa, Descabezado Grande–Cerro Azul, and Tatara–San Pedro. In the southernmost TSVZ and CSVZ, increase of $^{87}Sr/^{86}Sr$ with SiO_2 is rarely observed, and basaltic and evolved

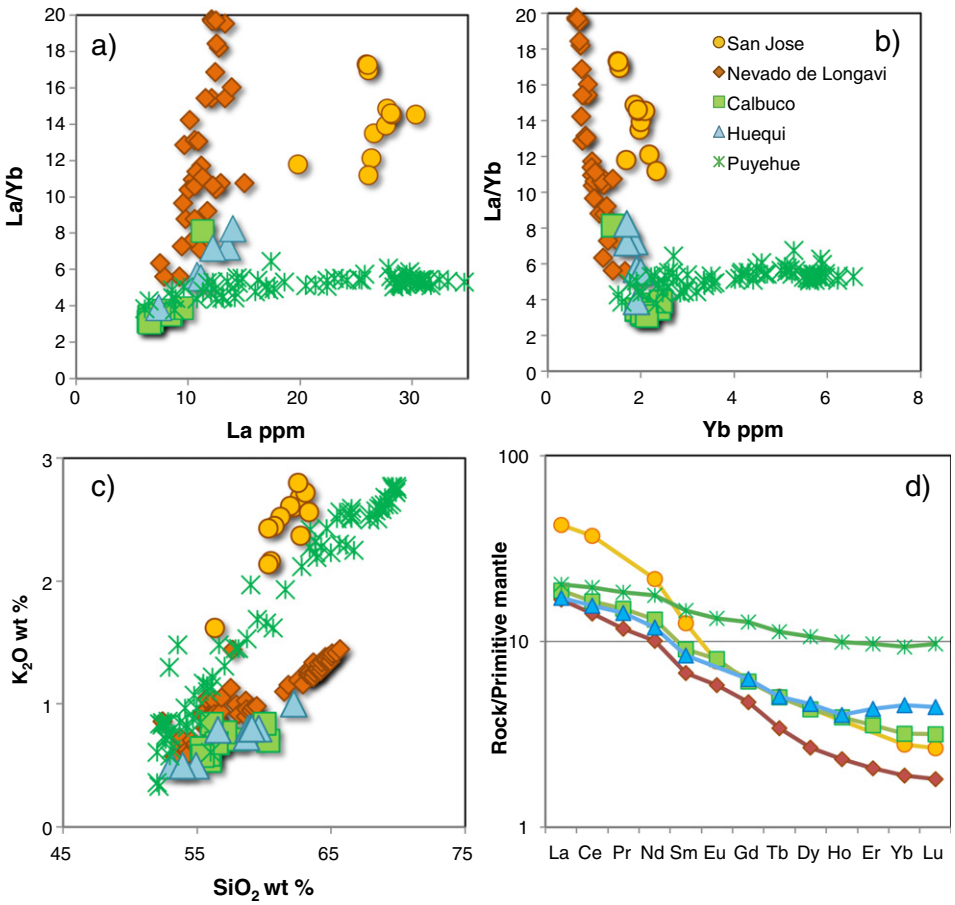

Fig. 12. a) La/Yb versus La and b) La/Yb versus Yb for amphibole-bearing suites from Nevado de Longaví, Calbuco, and Huequi, compared with hornblende-bearing andesites from San Jose (NSVZ). Basaltic andesites, andesites, and dacites are plotted. Puyehue is plotted for comparison as an example of an anhydrous suite; c) K_2O versus SiO_2 in hornblende-bearing or hornblende-affected suites compared with Puyehue, and d) typical REE patterns for each center; all samples have 58–60% SiO_2. Data are from sources in Fig. 3.

rocks from individual centers overlap, with total ranges of $^{87}Sr/^{86}Sr$ from <0.0001 to 0.0004 (Fig. 6). In the SSVZ, rhyolite from Chaiten has much higher $^{87}Sr/^{86}Sr$ than basaltic rocks from nearby Volcan Michinmahuida; other centers are too sparsely sampled to interpret conclusively.

Many researchers have argued that the lack of increase in Sr-isotope ratios in intermediate and felsic rocks in the SVZ does not preclude a role for crustal assimilation but reflects a lack of isotopic contrast between the basement rocks for assimilation and the magma (e.g., Dungan and Davidson, 2004). Basement in much of the CSVZ consists of Miocene or older plutonic rocks of arc origin (Parada et al., 2007). In other locations where isotopic contrast between basement and magma can be observed there are instances where high $^{87}Sr/^{86}Sr$ is correlated with SiO_2 (Fig. 6). For example, this occurs in the NSVZ as a whole, underlain by Mesozoic sedimentary sequences, in the TSVZ at Planchon-Peteroa, where Tertiary dolomitic limestone outcrops near the dacitic Azufre center (Holbik, 2014; Tormey et al., 1995), in andesites from Calbuco (CSVZ) and rhyolite from Chaiten (SSVZ), where outcropping basement includes schists and metasediments similar to the coastal Paleozoic accretionary complex (Herve et al., 2007). Since these rocks are not more fusible than granitoids, this observation supports the conclusion that overlapping $^{87}Sr/^{86}Sr$ in mafic and evolved rocks from the CSVZ does not necessarily reflect a lesser extent of crustal assimilation.

Elevated $\delta^{18}O$ compared with mantle values of 5–6 ‰ are also used to detect assimilation of sedimentary and metasedimentary rocks alone or coupled with $^{87}Sr/^{86}Sr$ (Deruelle et al., 1983; Harmon and Hoefs, 1984). This approach is problematic in the SVZ, where much of the uppermost basement consists of older volcanic sequences and plutonic rocks that have been hydrothermally altered. Studies in the SVZ demonstrated that such alteration results in low $\delta^{18}O$ (<5‰) so that their assimilation would produce anomalously low values in $\delta^{18}O$ (Grunder, 1987). In the SVZ, $\delta^{18}O$ values are scattered (Fig. 7), although high values (>7‰) are associated with high $^{87}Sr/^{86}Sr$, for example, in rhyolite from the NSVZ Diamante Caldera–Maipo Complex, andesites and dacites at northern TSVZ centers Palomo, Planchon–Peteroa, and Tatara–San Pedro, and in rhyolite from Chaiten in the SSVZ. Among basaltic SVZ rocks, $\delta^{18}O$ falls in the range 5.3–6.3‰, similar to mantle values, except at Cay and Maca (SSVZ) where they are higher (Fig. 7).

In the small eruptive centers near Villarrica, $\delta^{18}O$ values in basalts range from 5.6 to 6.0‰, typical of mantle-derived magma (Hickey-Vargas et al., 1989). An important characteristic of the LREE-enriched SEC is that $^{87}Sr/^{86}Sr$ ratios are low (0.7037–0.7039), some among the lowest in the SVZ (Fig. 6) and lower than in basalts from Villarrica stratovolcano (Fig. 14b). Together with other evidence, their low $^{87}Sr/^{86}Sr$ and $\delta^{18}O$ inconsistent with crustal assimilation as a cause of their LREE-enrichment.

4.3. Variation of $^{143}Nd/^{144}Nd$ and $^{176}Hf/^{177}Hf$ in the SVZ

Nd isotope ratios are broadly correlated with $^{87}Sr/^{86}Sr$ in the SVZ (Figs. 6 and 8). The most radiogenic values of $^{143}Nd/^{144}Nd$ = 0.51289–0.51291 are found in rocks at CSVZ volcanoes Llaima, Villarrica, and Puyehue. Lower values <0.51284 occur in the northern TSVZ (Descabezado Grande–Cerro Azul, Planchon–Peteroa, Tinguirririca), and the NSVZ (<0.51270). On a plot of $^{143}Nd/^{144}Nd$ vs $^{87}Sr/^{86}Sr$ (Fig. 14a), rocks from the CSVZ plot in a cluster, except for Osorno which has higher $^{87}Sr/^{86}Sr$, and Calbuco, which has higher $^{87}Sr/^{86}Sr$

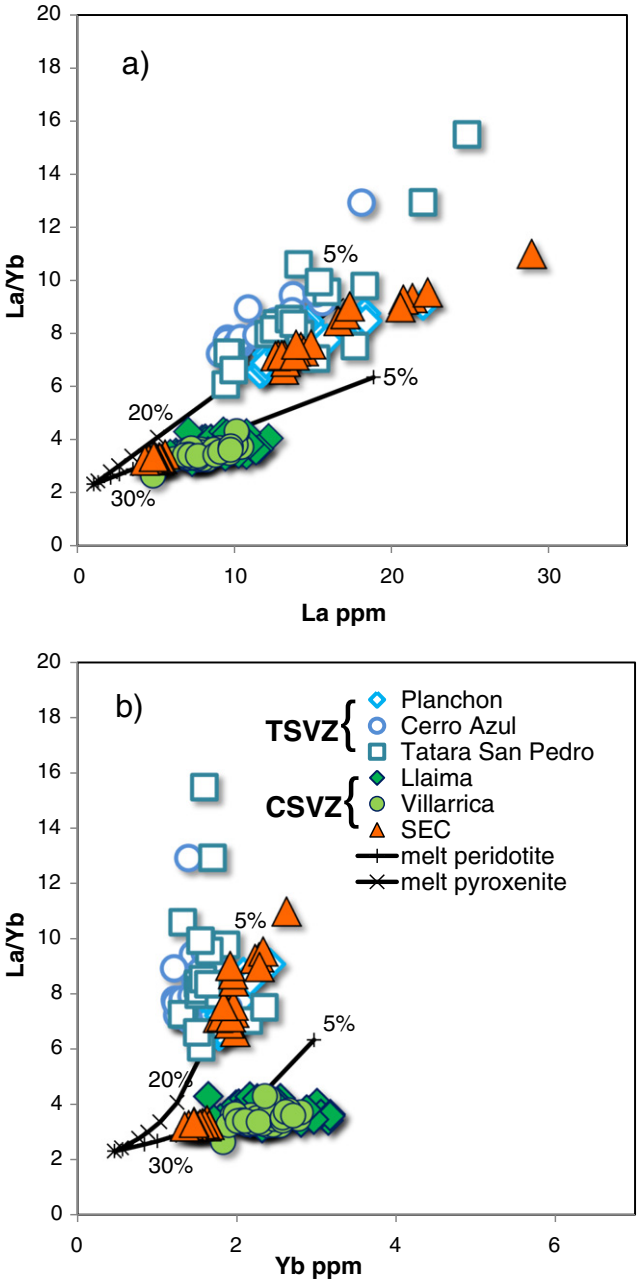

Fig. 13. a) La/Yb versus La and b) La/Yb versus Yb for basalts from small eruptive centers (SEC) near Villarrica, compared with TSVZ volcanoes Planchon–Peteroa, Cerro Azul, Tatara–San Pedro, and CSVZ volcanoes Villarrica and Llaima. Basalts and basaltic andesites only are shown. Curves show calculated compositions of primary melts of peridotite (60% olivine, 20% orthopyroxene, 15% clinopyroxene, and 5% spinel), and pyroxenite (20% olivine, 40% orthopyroxene, 30% clinopyroxene, and 10% spinel), having the REE concentrations of a mantle source for E-MORB (after Hickey-Vargas et al., 2016). Ticks marks show REE characteristics for 5%, 20%, and 30% melting. The diagram is scaled to Fig. 12 for comparison.

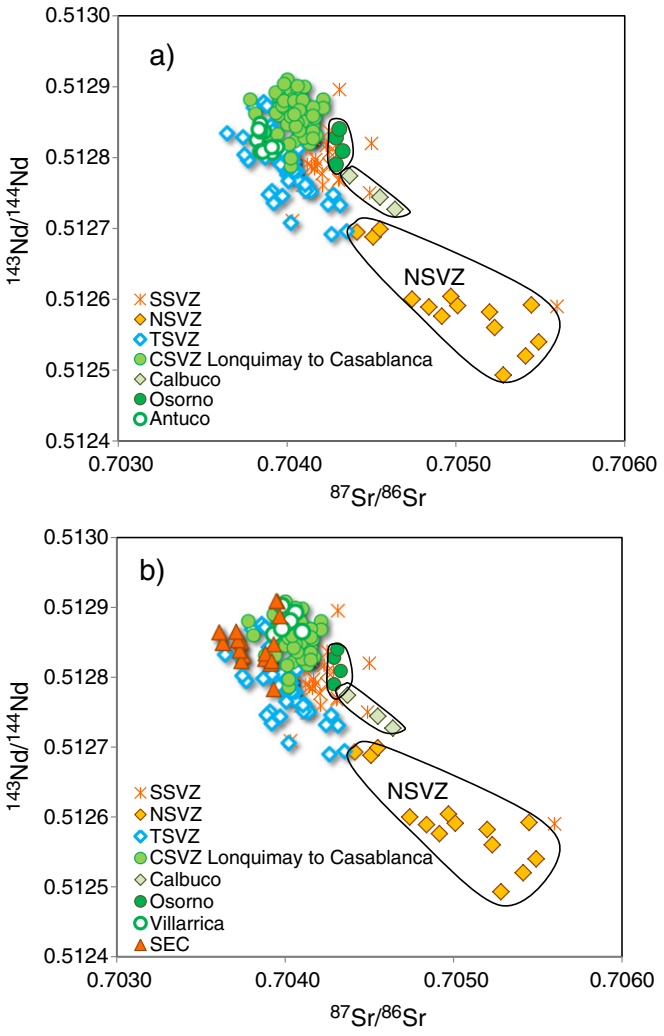

Fig. 14. a) $^{143}Nd/^{144}Nd$ versus $^{87}Sr/^{86}Sr$, showing characteristics of rocks from the different segments of the SVZ. Antuco is highlighted (open circles) because it plots with TSVZ volcanoes. b) $^{143}Nd/^{144}Nd$ versus $^{87}Sr/^{86}Sr$ showing the relationship between the small eruptive centers near Villarrica, Villarrica (open circles) and the field for TSVZ volcanoes and CSVZ rocks. Data are from sources listed for Fig. 6. Casablanca is part of the Antillanca Group at 40.8°S.

and lower $^{143}Nd/^{144}Nd$. Rocks from the TSVZ plot at slightly but consistently lower $^{87}Sr/^{86}Sr$ for a given $^{143}Nd/^{144}Nd$ ratio comparable to the CSVZ, including Osorno and Calbuco volcanoes. Rocks from the SSVZ are scattered, overlapping mostly with the CSVZ, except for Chaiten. NSVZ andesites and Chaiten rhyolite have the highest $^{87}Sr/^{86}Sr$ and lowest $^{143}Nd/^{144}Nd$ in the SVZ.

Fig. 9 shows the variation of ε_{Hf} versus ε_{Nd} in basaltic and intermediate SVZ volcanic rocks. Rocks from the TSVZ, CSVZ, and SSVZ plot in a field at slightly higher ε_{Hf} than the terrestrial and OIB–MORB mantle array correlation lines, while basaltic andesites from NSVZ volcano Casimiro plot at lower ε_{Hf} and ε_{Nd} on the terrestrial array, producing a slightly steeper slope for the SVZ as a whole. Samples from the SEC, Osorno, and Calbuco volcanoes, which define exceptions to the along-strike trend of Nd- and Sr-isotope ratios of SVZ volcanoes (Fig. 14a and b), do not stand out on this plot; Hf and Nd isotope ratios are closely correlated.

For the TSVZ and CSVZ, Jacques et al. (2013, 2014) attribute the along-strike variation of $^{143}Nd/^{144}Nd$, $^{176}Hf/^{177}Hf$, and $^{87}Sr/^{86}Sr$ to melting of relatively depleted and enriched mantle end members patterned on enriched and depleted South Atlantic MORB. Fig. 9 shows that rocks of the TSVZ, CSVZ, SSVZ plot in a linear trend at slightly lower ε_{Hf} for a given ε_{Nd} than the correlation line for South Atlantic MORB. Interestingly, Jacques et al. (2013, 2014) found that basalts from back arc locations in Argentina form a trend parallel to the SVZ volcanic front at systematically lower ε_{Hf} relative to ε_{Nd} (Fig. 9). They note that this relationship between arc and back arc volcanics is unusual and has not been found in other subduction settings. They propose that both mantle end members for the back arc array are within the South American Proterozoic subcontinental lithosphere, and distinct from those for the SVZ.

An important difference between the TSVZ and CSVZ is the lower $^{87}Sr/^{86}Sr$ for a given $^{143}Nd/^{144}Nd$ in basaltic rocks from the TSVZ. Based on ABS modeling, Jacques et al. (2014) attributed this pattern to

differing subduction zone parameters and mantle melting in the two segments. Primary melts in the TSVZ contain a slightly smaller quantity of slab component added to the mantle compared with the CSVZ, and the composition of the slab component is also more enriched in sediment compared with altered oceanic basalt. This, together with the original heterogeneity of enriched and depleted presubduction mantle asthenosphere, causes a range toward lower $^{87}Sr/^{86}Sr$ and $^{143}Nd/^{144}Nd$ in the TSVZ. A smaller extent of melting also occurs in the TSVZ as the result of the reduced slab component. All of these parameters are well-established controls on the composition of subduction magmas (Elliott and Eiler, 2003; Plank and Langmuir, 1993; Turner and Langmuir, 2015a, 2015b) and applicable to the scale of the SVZ as a whole.

Fig. 14b shows the Villarrica region SEC superimposed on the SVZ diagram of $^{143}Nd/^{144}Nd$ versus $^{86}Sr/^{86}Sr$. More LREE-enriched SEC and less LREE-enriched SEC basalts fall separately in fields for the TSVZ and for the CSVZ, respectively. The LREE-enriched SEC have uniformly lower $^{87}Sr/^{86}Sr$ and $^{143}Nd/^{144}Nd$ than basalts from Villarrica, therefore isotopic differences between the two groups of SEC basalts parallel the differences between TSVZ and CSVZ basalts. As noted by Hickey-Vargas et al. (1989, 2002), it is difficult to attribute such differences to changes in subduction zone parameters because this would require ascent of distinct subduction components through the convecting and partially molten asthenosphere over a small spatial scale (<20 km^2) and short (<10,000 y) timescale. Based on this consideration, a source for geochemical differences within the mantle lithosphere was preferred.

A different explanation for systematic geochemical differences between basaltic magmas of the TSVZ and CSVZ was proposed by Holbik (2014). He compared calculated depths of primary magma separation from mantle peridotite with the modeled lithospheric structure of the SVZ (Fig. 2). Using basalts with petrologic features consistent with being near-liquids from TSVZ and CSVZ volcanoes, temperatures and depths of magma separation were calculated over a range of H_2O and fO_2 conditions using the thermobarometer of Lee et al. (2009). Results revealed that depths of magma extraction were remarkably consistent across the TSVZ and CSVZ, between 47 and 53 km, averaging 50 km. These depths are all within the regional mantle lithosphere (Fig. 2). Because the crust thickens in the TSVZ (Fig. 2), such depths are near the Moho; in the CSVZ, they are 10–15 km below the Moho. Consequently, asthenosphere-derived magma might interact more with the lower crust in the TSVZ than in the CSVZ (Fig. 17), resulting in lower $^{143}Nd/^{144}Nd$, $^{176}Hf/^{177}Hf$, and $^{87}Sr/^{86}Sr$ compared with the CSVZ. Holbik (2014) also proposed that the separation depths might define a shallower local, sub-volcanic lithosphere–asthenosphere boundary, as suggested by geophysical findings at 39.5°S in the SVZ (Thorwart et al., 2014)

4.4. Variation of Pb-isotope ratios in the SVZ

As shown in Figs. 10 and 15, Pb-isotope ratios do not vary systematically along-strike in lavas of the volcanic front in the SVZ; $^{206}Pb/^{204}Pb$ in basaltic rocks varies from 18.47 to 18.64. There are, however, local variations which may reflect crustal and mantle processes. For example, rhyolite from Chaiten and andesite from Palomo both have high $^{87}Sr/^{86}Sr$ and $\delta^{18}O$, probably reflecting assimilation of upper crust, and higher $^{206}Pb/^{204}Pb$, $^{207}Pb/^{204}Pb$, and $^{208}Pb/^{204}Pb$ than the rest of the SVZ (Figs. 10 and 15). This suggests that assimilated crust was more radiogenic than other volcanic front magmas. Lowest Pb-isotope ratios are found in basaltic andesites from Hudson and Cay in the SSVZ, close to the subducting Chile Rise, which could be related to an increased input of Pb derived from hydrothermally altered subducted basalt. Overall, SVZ Pb-isotope ratios plot within the field for Nazca plate sediment, and overlap with fields for Chile trench and river mouth sediment (Hildreth and Moorbath, 1988; Lucassen et al., 2010; Jacques et al., 2013) and the field for Tertiary intrusive rocks from the volcanic arc basement (37°–40°S latitude; Lucassen et al. 2004). Mesozoic and Paleozoic intrusive and metamorphic rocks which could be involved in SVZ magmatism through crustal assimilation or subduction erosion, plot in a large fields encompassing all of these sources, although predominantly at higher $^{207}Pb/^{204}Pb$ for a given $^{206}Pb/^{204}Pb$ or $^{208}Pb/^{204}Pb$ (Lucassen et al., 2004).

In contrast to the subdued along-strike variation in Pb-isotopes in the SVZ, Jacques et al. (2013, 2014) found a striking trend from the SVZ field toward lower $^{206}Pb/^{204}Pb$ among basalts from back arc locations in Argentina (Fig. 15). Pb-isotope values for these basalts approach those of South Atlantic MORB and are correlated with decreasing Pb/REE enrichment, approaching mantle values. In their ABS-based quantitative model, they estimate that CSVZ and TSVZ magmas contain from about 0.5–3% of a Pb-rich subduction component derived from AOC (40%) and trench sediment (60%), which is added to enriched and depleted South Atlantic MORB sources. Back arc basalts have little subduction component, thus their $^{206}Pb/^{204}Pb$ and Pb/REE are lower. In this model, with fixed values for end members, the variation of $^{206}Pb/^{204}Pb$ in SVZ volcanic front lavas is produced by mixing between mantle and subduction components.

Another possible reason for this variation that the sources of Pb in volcanic front magmas have varying Pb-isotope ratios. For example, fields for Chile trench sediments and for Tertiary intrusive rocks both form elongate fields which overlap and parallel those of the SVZ on plots of $^{208}Pb/^{204}Pb$ and $^{207}Pb/^{204}Pb$ versus $^{206}Pb/^{204}Pb$ (Fig. 15). SVZ magmas may inherit that variation through the sediment end member of a subduction component. Alternatively, Pb-isotopes may be overprinted by assimilation of Tertiary intrusive rocks, with little impact on Sr, Nd, Hf, or O-isotopes. Finally, the fact that trench sediments are largely composed of eroded upper crustal materials from the SVZ, with a large component of erodible volcanic material (Voelker et al., 2013), suggests the variation could reflect a steady state Pb-isotope range cycled between arc volcano sources and predominantly subducted volcanic arc sediment. High-resolution Pb-isotope studies, coupled with $^{10}Be/^{9}Be$, focused on individual volcanic centers may be able distinguish such crustal and subducted sources.

4.5. U-series disequilibrium, $^{10}Be/^{9}Be$ and Th/La

The geochemical parameters ($^{238}U/^{230}Th$), $^{10}Be/^{9}Be$, and B/Be can provide unequivocal evidence for input from the subducted Nazca plate and to understand the variation in such inputs (Hickey-Vargas et al., 2002; Morris et al., 1990; Sigmarsson et al., 1990, 2002). Fig. 11 shows the extent of ($^{238}U/^{230}Th$) disequilibrium and $^{10}Be/^{9}Be$ in SVZ lavas ranging from basalt to rhyolite. Maximum ^{238}U enrichment or excess (in this case expressed as the deviation of ($^{238}U/^{232}Th$) from the equiline value at the same ($^{230}Th/^{232}Th$)) of up to +0.4 occurs only in basalt and basaltic andesite in the CSVZ, at volcanoes Llaima, Villarrica, and Osorno, whereas mafic rocks from Puyehue (CSVZ), centers to the north (e.g., Antuco) and most andesites, dacites, and rhyolites show lower values, and occasional ^{230}Th enrichment.

Because ^{226}Ra has a half-life of 1600 y, ($^{226}Ra/^{230}Th$) disequilibrium is useful for understanding the timing of subduction zone processes (e.g., Turner et al., 2003, 2006), specifically the time between addition of ^{226}Ra-rich slab fluids and magma eruption. Sigmarsson et al. (2002) found that basaltic rocks from historic eruptions of CSVZ volcanoes Osorno, Mocho, Villarrica, Lonquimay and Antuco have differing ($^{226}Ra/^{230}Th$) greater than 1, whereas lavas erupted at the more northerly volcanoes, Nevados de Chillan and San Jose, are in secular equilibrium. Rocks from the CSVZ volcanoes as a group also showed a strong correlation between $^{10}Be/^{9}Be$ and ($^{226}Ra/^{230}Th$), suggesting recent enrichment of mantle sources by sediment-derived materials. ($^{231}Pa/^{235}U$) disequilibrium was studied in the SVZ at Llaima Volcano (Reubi et al., 2011). ^{231}Pa (half-life = 32,760 y) is an indicator of source depletion/fertility and melting conditions rather than fluid addition and ($^{231}Pa/^{235}U$) disequilibrium is strongly dependent on residual

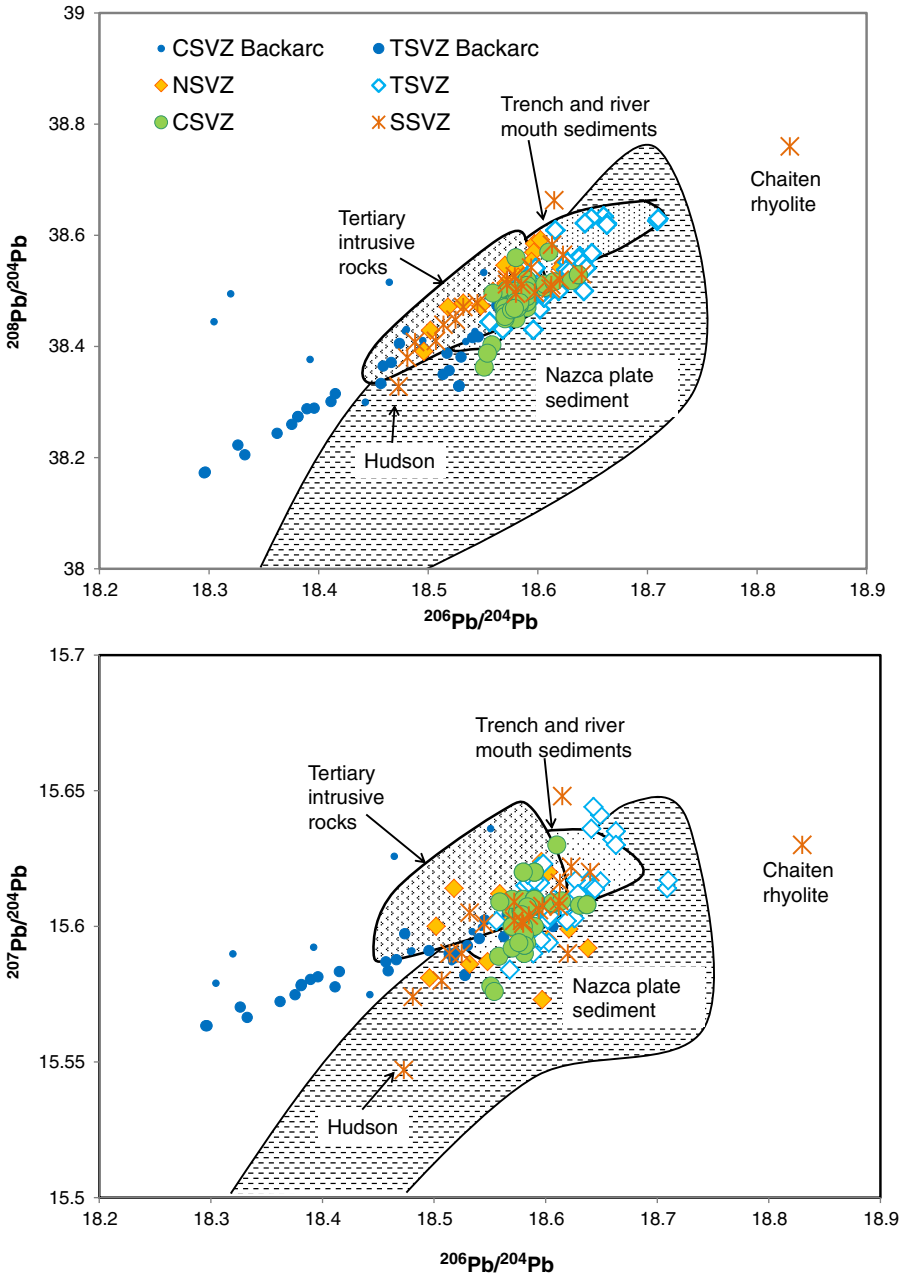

Fig. 15. Plot of $^{208}Pb/^{204}Pb$ and $^{207}Pb/^{204}Pb$ versus $^{206}Pb/^{204}Pb$, showing volcanic rocks from the SVZ. SVZ data are from sources listed for Fig. 9. Data for back arc basalts are from Jacques et al. (2013, 2014) and Holm et al. (2014). The field for Nazca plate sediments is constructed with data from Dasch (1981). Data for trench sediments are from Lucassen et al. (2010), Jacques et al. (2013), and Hildreth and Moorbath (1988). Data for Tertiary intrusive rocks are from Lucassen et al. (2004).

mineralogy (Stracke et al., 2006). Llaima samples show excess ^{231}Pa, as is common in most subduction systems (Turner et al., 2006).

The tendency for evolved lavas to approach ($^{238}U/^{230}Th$) secular equilibrium, even when mafic precursors exhibit disequilibrium, has been widely noted in volcanic systems (e.g., Reagan et al., 2003). Explanations include long-term storage of differentiated silicic melt in crystal mushes within the crust, alone or together with assimilation of older crustal rocks at secular equilibrium (Reagan et al., 2003; Reubi et al., 2011; Ruprecht and Cooper, 2012). In a recent study of lavas from Llaima volcano, Reubi et al. (2011) found that ($^{230}Th/^{238}U$/) in basaltic andesites increased toward equilibrium from low values similar to those for basalts from Villarrica and Osorno, with increasing Th/La ratios and SiO_2 (Fig. 16). Their interpretation is that the basaltic magmas assimilated small amounts (10%) of partial melts or bulk older granitoid basement rocks. Since Llaima is in an area of the SVZ where there is little apparent contrast between magma and basement for long-lived radiogenic isotopes $^{87}Sr/^{86}Sr$ and $^{143}Nd/^{144}Nd$, this is a viable conclusion. The critical aspect of the finding is that the diminishing disequilibrium signal occurred among lavas that are relatively mafic (Fig. 16), underscoring the necessity to identify the impact of crustal processes before using U-series isotopes to infer subduction zone mantle processes. An important conclusion is that basaltic rocks with low Th/La and SiO_2, within related suites of basalt and basaltic andesite, are most likely to reflect subduction zone contributions.

Volcanic rocks from Puyehue show the opposite relationship; although dacitic and rhyolitic rocks have ($^{238}U/^{230}Th$) closest to 1, some basalts show slight ^{230}Th excesses (Figs. 11 and 16). Jicha et al. (2007) interpreted that the ^{230}Th excesses resulted from both a smaller than normal input of subducted fluid borne U and subsequent interaction of mafic magma with lower crustal rocks. Similar to the case of Llaima,

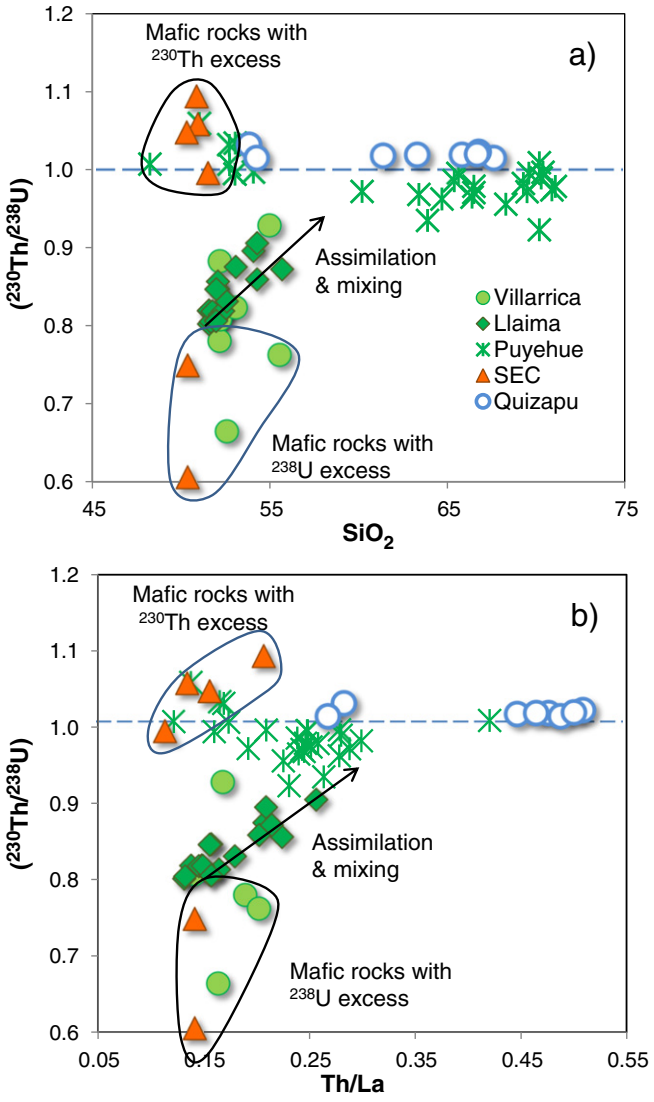

Fig. 16. a) (^{230}Th/^{238}U) versus SiO_2 and b) (^{230}Th/^{238}U) versus Th/La in volcanic rocks from volcanic front stratovolcanoes and SEC basalts. Two groups of mafic rocks are defined, with crustal impacts indicated by increasing SiO_2, Th/La, and secular equilibrium. Data are from sources in Fig. 11.

interaction with old crustal rocks may diminish disequilibrium. Minerals such as magnetite or zircon are residual phases in crustal rocks that could produce a Th-excess (Jicha et al., 2007). For the evolved rocks, crustal assimilation and fractionation of U and Th by differentiating minerals, possibly apatite, was also proposed to explain their variable U excesses.

As noted above, Villarrica SEC show a variation of (^{238}U/^{230}Th), (^{226}Ra/^{230} Th) and ^{10}Be/^{9}Be characteristics that is correlated with LREE/HREE (Hickey-Vargas et al., 2002). Type 1 SEC basalts with low LREE/HREE, similar to Villarrica basalts, exhibit large ^{238}U and ^{226}Ra excesses, and higher ^{10}Be/^{9}Be (4.6×10^{-11}). Type 2 SEC with high LREE/HREE display secular equilibrium or slight ^{230}Th enrichment, (^{226}Ra/^{230}Th) at equilibrium, and lower ^{10}Be/^{9}Be ($1.5–1.9 \times 10^{-11}$). Hickey-Vargas et al. (2002, 2016), proposed that near-equilibrium (^{238}U/^{230}Th) correlated with high LREE/HREE in the small area of the SEC results from interaction of ambient sub-SVZ asthenospheric melt with aged subduction-related pyroxenite in the mantle lithosphere. For Puyehue Volcano (Fig. 16), it is plausible that similar interaction of magma with pyroxenite in the mantle lithosphere produced a variety of primary basaltic magmas, including some with ^{238}U excesses, which then differentiated to form the more silicic rocks (Fig. 16). Jicha et al. (2007) hypothesized that both mantle melting processes and interaction with the lower crust might produce the variation of La/Yb and U-series characteristics of Puyehue basalts. Magmas having large inputs of subducted materials would melt more and have low La/Yb and (^{238}U/^{230}Th) > 1, and then be variably overprinted by lower crustal melts leading to high La/Yb and (^{238}U/^{230}Th) <1.

5. Synthesis of small- and large-scale trends

5.1. Overview of magma generation in the TSVZ and CSVZ

Most along-strike geochemical trends defined by early research on TSVZ and CSVZ volcanic centers have been validated with additional geochemical data. However, there is continuing controversy over whether predominantly mantle melting and subduction inputs (Jacques et al., 2013, 2014), or interaction of magma with the mantle lithosphere and crust are responsible for those changes (Dungan et al., 2001; Dungan and Davidson, 2004; Reubi et al., 2011). In our comparison of small-scale and large-scale geochemical variations in the SVZ, we find that most systematic geochemical differences between basaltic rocks from TSVZ and CSVZ volcanoes are paralleled in differences among contemporaneous monogenetic basaltic SEC associated with the LOFS near Villarrica (Figs. 13, 14, 16). This means that all of the sources and conditions needed to produce those variations occur within a 20 km^2 area of the sub-SVZ crust, mantle, and slab. Using the Type 1 and Type 2 classification of López-Escobar et al. (1995a), and comparing the TSVZ with the CSVZ, we observe that Type 1 basalts have not been found in the TSVZ whereas both Type 1 and Type 2 are found in the CSVZ, with Type 2 normally found in SEC along the LOFS. Analysis of the stress regimes related to the LOFS indicate that the location of stratovolcanoes and SEC are controlled by the fault system and that it is a probable network for magma ascent through the crust (Cembrano and Lara, 2009; López-Escobar et al., 1995a). Therefore, we propose that a major control on the geochemical differences between the TSVZ and CSVZ is that a greater range of magma types, ranging from ambient asthenospheric melts (Type 1) to melts that have interacted with mantle lithosphere (Type 2), are able to reach the surface in the CSVZ due to the increased crustal permeability created by the LOFS. For Villarrica region Type 2 SEC, high LREE/HREE, low ^{87}Sr/^{86}Sr, and ^{143}Nd/^{144}Nd was attributed to interaction of magma with pyroxenite in the mantle lithosphere. That pyroxenite was inferred to form from subduction-related magma reacting with the peridotite of the mantle lithosphere over the >300 Ma history of subduction along western South America (Hickey-Vargas et al., 2016). For the TSVZ, this could also be the case; ambient asthenospheric melts rise and interact with the mantle lithosphere and become enriched. Alternatively, the Type 2 characteristics of TSVZ basaltic magmas could be attributed to a smaller extent of mantle partial melting. As noted by Jacques et al. (2013, 2014), this is consistent with the lower eruption rates and lower magma production rates observed for the TSVZ compared with the CSVZ (Voelker et al., 2011). A further possibility is that geochemical differences reflect differing presubduction enrichment of the asthenospheric mantle (Jacques et al., 2013, 2014). If the Type 2 characteristics are attributed mainly to interaction of a relatively uniform asthenospheric melt with pyroxenite in the lithosphere, then all TSVZ magmas have undergone some interaction, as the result of low crustal permeability there, whereas interaction is low to variable in the CSVZ. Our preferred interpretation is that the presence of the LOFS in the CSVZ is a primary factor influencing the type of magma that reaches the upper crust and is erupted and that magma generation processes in the slab/asthenosphere system may be, but are not necessarily, similar in the TSVZ and CSVZ (Fig. 17). Corroboration of similar magma generation processes would be the finding of primitive Type 1 basaltic magmas with high values for transient subduction tracers in the TSVZ under conditions of unusual crustal permeability.

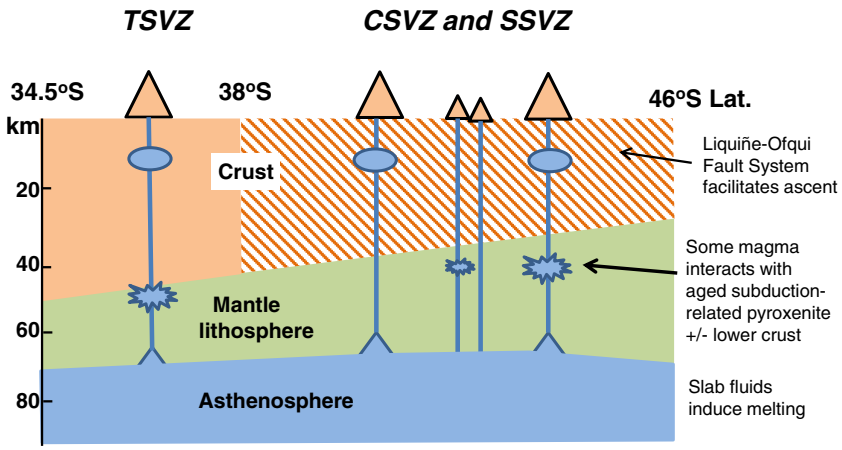

Fig. 17. Schematic along-strike cross-section of the SVZ from 34.5°S to 46°S (TSVZ, CSVZ, and SSVZ), showing the extent of the LOFS (diagonal lines) and its proposed influence on magma ascent. Magma in all segments is generated by addition of slab-derived fluid to the asthenosphere accompanied by melting and ascent. In the TSVZ, magma interacts with mantle lithosphere and crust because ascent is not facilitated by the LOFS. In the CSVZ, magmatic ascent is facilitated by the LOFS, and diverse magma types reach the surface. These include unaltered melts of subduction-modified asthenosphere and magmas that interact with the lithosphere, like those of the TSVZ.

5.2. Geologic and geochemical reassessment of segments

Based on the along-strike geochemical variations shown in Figs. 4-11, together with recognition of the LOFS as a possible primary factor influencing magma ascent in the SVZ, we propose a more southerly position of the boundary of the CSVZ to 38°S rather than 37°S (Fig. 1; Fig. 17), specifically between Lonquimay/Tolguaca volcanoes and Callaquen Volcano, at the northern extremity of the LOFS. Basaltic rocks from Antuco Volcano (37.4°S) and Callaquen (37.9°S) plot with the TSVZ in isotopic character and La/Yb ratios (Figs. 5–10, 14). Detailed study of Callaquen may elucidate whether there is a shift in magma character related to changes in crustal stress state at that point in the SVZ. We also note that there does not seem to be any fundamental difference in the range of geochemical characteristics of volcanoes from the CSVZ and the SSVZ, except possibly for Hudson Volcano (Figs. 5-8, 10), which is generally consistent with the concept that the LOFS is a key feature in geochemical segmentation of the arc.

6. Conclusions

We reviewed along-strike variations of isotopic and trace element parameters in mafic lavas of volcanic front volcanoes in the SVZ and examined models for their origin.

Volcanoes of the NSVZ are mainly andesitic and the most mafic rocks are basaltic andesites. These typically have higher $^{87}Sr/^{86}Sr$, lower $^{143}Nd/^{144}Nd$, lower $^{176}Hf/^{177}Hf$, and higher La/Yb (11–28) compared with volcanoes south of 34.5°S in the TSVZ, CSVZ, and SSVZ. Interpretations of their origin concur that incorporation of continental crust is important, but crust may be added by 1) assimilation during magma ascent from a subduction-modified asthenosphere or 2) by subduction erosion of the Andean forearc crust and melting of subducted crust within the sub-arc asthenosphere. Geochemical parameters do not conclusively distinguish these processes, and both are supported by geologic arguments, such as evidence for retreat of the continental margin through time and evidence for thick continental crust.

Volcanoes of the TSVZ are mainly basaltic andesite, with rare basalt, and common andesite and dacite. Basaltic lavas typically have higher and more variable La/Yb (5–16) and lower $^{87}Sr/^{86}Sr$ for given $^{143}Nd/^{144}Nd$ than those of the CSVZ. $^{143}Nd/^{144}Nd$ and $^{176}Hf/^{177}Hf$ are closely correlated in both TSVZ and CSVZ basaltic rocks. TSVZ lavas have low values of time-sensitive tracers of subduction inputs such as high ($^{238}U/^{230}Th$) and $^{10}Be/^{9}Be$. These differences between the TSVZ and CSVZ could indicate 1) a greater contribution of hydrous subduction zone fluids and fluid mobile elements to the asthenosphere beneath CSVZ volcanic front volcanoes, triggering greater extents of melting, or 2) greater interaction of TSVZ subduction-modified asthenospheric magmas with the continental lithosphere during ascent. An important constraint on these hypotheses is that the geochemical characteristics of both CSVZ and TSVZ mafic lavas are found together in the CSVZ within a 20 km^2 cluster of monogenetic basaltic cones aligned with the Liquiñe–Ofqui Fault System. Based on this observation, we conclude that a major influence on the along-strike change in magma geochemistry from the TSVZ to the CSVZ is the enhanced permeability of the lithosphere provided by the LOFS which extends from 38°S to 46°S. In the TSVZ, and for Type 2 monogenetic basaltic cones, magma ascending from the asthenosphere is overprinted by interaction with pyroxenite in the lithospheric mantle (Fig. 17), leading to higher La/Yb and dilution of time-sensitive subduction tracers such as high ($^{238}U/^{230}Th$) and $^{10}Be/^{9}Be$, in addition to their other geochemical differences.

In the CSVZ, where volcano locations are controlled by the LOFS, magma ascent through the lithosphere is facilitated. Many CSVZ stratovolcano magmas rise directly from the actively subduction-modified asthenosphere into the crust, while others (Type 2 SEC and minor episodic contributions to stratovolcanoes) interact with mantle lithosphere pyroxenite as they ascend (Fig. 17). CSVZ stratovolcanoes show clear evidence of recent subduction inputs, high ($^{238}U/^{230}Th$) and $^{10}Be/^{9}Be$, and have lowest La/Yb (2–7 in basalts) in the SVZ. Because of greater upper plate overprinting in the TSVZ, it is difficult to discern whether there are also along-strike differences in the composition of slab fluids, for example, changes in the relative contribution of sediment and altered oceanic crust, or in the composition of mantle sources or the extent of mantle melting between the TSVZ and CSVZ.

Lavas from SSVZ volcanoes are less well-characterized than those of the CSVZ. Geochemical features of basaltic magmas in the SSVZ are similar to those of the CSVZ: La/Yb < 7 in most basalts, and higher $^{87}Sr/^{86}Sr$ for a given $^{143}Nd/^{144}Nd$ compared with the TSVZ. Given the importance of the LOFS as a pathway for magma ascent, we conclude that SSVZ magmas are generated from subducted and mantle source materials similar to those of the CSVZ, with variable interaction with the mantle lithosphere. Possible exceptions are volcanoes Hudson and Cay, which have lower $^{206}Pb/^{204}Pb$, $^{207}Pb/^{204}Pb$, and $^{208}Pb/^{204}Pb$ than magmas of the CSVZ. These centers are close to the Chile Rise, where subduction fluids may include more Pb from hydrothermally altered basaltic crust.

Volcanoes Nevado de Longavi (36.2°S, TSVZ), Calbuco (41.3°S, CSVZ) and Huequi (42.4°S, SSVZ) are unique in having geochemical evidence for hornblende and possibly garnet fractionation from mafic magmas. One hypothesis is that fracture zones on the Nazca plate may deliver

more water to the sub-arc asthenosphere at these volcanoes than adjacent areas, resulting in unusually high water contents in primitive basaltic magmas and stabilization of hornblende as a liquidus phase. This pattern is weakly expressed geographically; Nevado de Longavi and Calbuco overlie fracture zones, but Huequi does not, and other volcanoes, such as Villarrica and Yanteles overlie fracture zones and lack hydrous minerals.

SVZ magmas residing in the upper crust undergo a wide array of assimilative processes, many of which are hidden by the lack of contrast between crust and magma for long-lived radiogenic isotopes and $\delta^{18}O$. These have been detected by detailed U-series disequilibrium studies which show that extended crustal residence causes produced ($^{238}U/^{230}Th$) close to secular equilibrium and can be linked to related trace element signatures such as increasing Th/La as a sign of assimilation. These studies imply that mildly increasing SiO_2 content, coupled with diminishing disequilibrium, together with associated trace element ratios, are good indicators for discerning the impacts of upper crustal assimilation on the composition of mafic magma.

Supplementary data to this article can be found online at http://dx.doi.org/10.1016/j.lithos.2016.04.014.

Acknowledgments

RH-V gratefully acknowledges support from National Science Foundation grant EAR 0337483 enabling this work. We acknowledge many contributions by the late *L. Lopez Escobar* to the scientific development of ideas presented in this work, as well as contributions selecting and documenting volcanic rock samples from field sites throughout Chile. We thank Charles Stern and an anonymous reviewer for many helpful comments and observations which led to improvement of the manuscript.

References

Alonso-Perez, R., Müntener, O., Ulmer, P., 2009. Igneous garnet and amphibole fractionation in the roots of island arcs: experimental constraints on andesitic liquids. Contributions to Mineralogy and Petrology 157, 541–558.
Anderson, M., Alvarado, P., Zandt, G., Beck, S., 2007. Geometry and brittle deformation of the subducting Nazca Plate, Central Chile and Argentina. Geophysical Journal International 171, 419–434.
Cembrano, J., Lara, L., 2009. The link between volcanism and tectonics in the Southern Volcanic Zone of the Chilean Andes; a review. Tectonophysics 471, 96–113.
Cembrano, J., Herve, F., Lavenu, A., 1996. The Liquiñe Ofqui fault zone; a long-lived intra-arc fault system in southern Chile. Tectonophysics 259, 55–66.
Cembrano, J., Schermer, E., Lavenu, A., Sanhueza, A., 2000. Contrasting nature of deformation along an intra-arc shear zone, the Liquiñe–Ofqui fault zone, southern Chilean Andes. Tectonophysics 319, 129–149.
Chauvel, C., Lewin, E., Carpentier, M., Arndt, N., Marini, J.-C., 2008. Role of recycled oceanic basalt and sediment in generating the Hf–Nd mantle array. Nature Geoscience 1, 64–67.
Costa, F., Singer, B., 2002. Evolution of Holocene dacite and compositionally zoned magma, Volcan San Pedro, Southern Volcanic Zone, Chile. Journal of Petrology 43, 1571–1593.
Costa, F., Dungan, M.A., Singer, B.S., 2002. Hornblende- and phlogopite-bearing gabbroic xenoliths from Volcan San Pedro (36 degrees S), Chilean Andes; evidence from melt and fluid migration and reactions in subduction-related plutons. Journal of Petrology 43, 219–241.
Dasch, E.J., 1981. Lead isotopic composition of metalliferous sediments from the Nazca Plate. Memoir - Geological Society of America 154, 199–209.
Davidson, J.P., Dungan, M.A., Ferguson, K.M., Colucci, M.T., 1987. Crust-magma interactions and the evolution of arc magmas; the San Pedro–Pellado volcanic complex, southern Chilean Andes. Geology (Boulder) 15, 443–446.
Davidson, J.P., Ferguson, K.M., Colucci, M.T., Dungan, M.A., 1988. The origin and evolution of magmas from the San Pedro Pellado volcanic complex, S. Chile; multicomponent sources and open system evolution. Contributions to Mineralogy and Petrology 100, 429–445.
Davidson, J., Turner, S., Handley, H., Macpherson, C., Dosseto, A., 2007. Amphibole "sponge" in arc crust? Geology (Boulder) 35, 787–790.
DeMets, C., Gordon, R.G., Argus, D.F., 2010. Geologically current plate motions. Geophysical Journal International 181, 1–80.
Deruelle, B., Harmon, R.S., Moorbath, S., 1983. Combined Sr–O isotope relationships and petrogenesis of Andean volcanics of South America. Nature (London) 302, 814–816.
D'Orazio, M., Innocenti, F., Manetti, P., Tamponi, M., Tonarini, S., Gonzalez Ferran, O., Lahsen, A., Omarini, R., 2003. The Quaternary calc–alkaline volcanism of the Patagonian Andes close to the Chile triple junction; geochemistry and petrogenesis of volcanic rocks from the Cay and Maca Volcanoes (approximately 45 degrees S, Chile). Journal of South American Earth Sciences 16, 219–242.
Dungan, M.A., 2005. Partial melting and the earth's surface: implications for assimilation rates and mechanisms in subvolcanic intrusions. Journal of Volcanology and Geothermal Research 140, 193–203.
Dungan, M.A., Davidson, J., 2004. Partial assimilative recycling of the mafic plutonic roots of arc volcanoes; an example from the Chilean Andes. Geology (Boulder) 32, 773–776.
Dungan, M.A., Wulff, A., Thompson, R.A., 2001. Eruptive stratigraphy of the Tatara–San Pedro Complex, 36 degrees S, Southern Volcanic Zone, Chilean Andes; reconstruction method and implications for magma evolution at long-lived arc volcanic centers. Journal of Petrology 42, 555–626.
Dzierma, Y., Thorwart, M., Rabbel, W., 2012a. Moho topography and subducting oceanic slab of the Chilean continental margin in the maximum slip segment of the 1960 Mw 9.5 Valdivia (Chile) earthquake from P-receiver functions. Tectonophysics 530-531, 180–192.
Dzierma, Y., Rabbel, W., Thorwart, M., Koulakov, I., Wehrmann, H., Hoernle, K., Comte, D., 2012b. Seismic velocity structure of the slab and continental plate in the region of the 1960 Valdivia (Chile) slip maximum; insights into fluid release and plate coupling. Earth and Planetary Science Letters 331-332, 164–176.
Elliott, T., Eiler, J.M., 2003. Tracers of the slab. Geophysical Monograph 138, 23–45.
Feeley, T.C., Dungan, M.A., 1996. Compositional and dynamic controls on mafic-silicic magma interactions at continental arc volcanoes; evidence from Cordon El Guadal, Tatara-San Pedro Complex, Chile. Journal of Petrology 37, 1547–1577.
Feeley, T.C., Dungan, M.A., Frey, F.A., 1998. Geochemical constraints on the origin of mafic and silicic magmas at Cordon El Guadal, Tatara-San Pedro Complex, central Chile. Contributions to Mineralogy and Petrology 131, 393–411.
Ferguson, K.M., Dungan, M.A., Davidson, J.P., Colucci, M.T., 1992. The Tatara-San Pedro Volcano, 36 degrees S, Chile; a chemically variable, dominantly mafic magmatic system. Journal of Petrology 33, 1–43.
Fierstein, J., Bruggman, P.E., Bartel, A.J., Stewart, K.C., Taggart Jr., J.E., Drake, R.E., Hildreth, W., 1989. Chemical analyses of rocks and sediments from central Chile. Open-File Report - U.S.Geological Survey.
Futa, K., Stern, C.R., 1988. Sr and Nd isotopic and trace element compositions of Quaternary volcanic centers of the Southern Andes. Earth and Planetary Science Letters 88, 253–262.
Gerlach, D.C., Frey, F.A., Moreno-Roa, H., Lopez-Escobar, L., 1988. Recent volcanism in the Puyehue–Cordon Caulle region, Southern Andes (40.5°S): petrogenesis of evolved lavas. Journal of Petrology 29, 333–382.
Grove, T.L., Baker, M.B., 1984. Phase equilibrium controls on the tholeiitic versus calc-alkaline differentiation trends. Journal of Geophysical Research 89, 3253–3274.
Grunder, A.L., 1987. Low delta $^{18}0$ silicic volcanic rocks at the Calabozos Caldera Complex, Southern Andes; evidence for upper-crustal contamination. Contributions to Mineralogy and Petrology 95, 71–81.
Gutierrez, F., Gioncada, A., Gonzalez Ferran, O., Lahsen, A., Mazzuoli, R., 2005. The Hudson Volcano and surrounding monogenetic centres, Chilean Patagonia; an example of volcanism associated with ridge-trench collision environment. Journal of Volcanology and Geothermal Research 145, 207–233.
Harmon, R.S., Hoefs, J., 1984. Oxygen Isotope Ratios in Late Cenozoic Andean Volcanics. Shiva Publ., Nantwich, Nantwich, United Kingdom (GBR), pp. 9–20.
Hayes, G.P., Wald, D.J., Johnson, R.L., 2012. Slab 1.0: A three-dimensional model of global subduction zone geometries. Journal of Geophysical Research B01302. http://dx.doi.org/10.1029/2011JB008524.
Herve, F., Faundez, V., Calderon, M., Massonne, H., Willner, A.P., 2007. Metamorphic and Plutonic Basement Complexes. The Geological Society, London, London, United Kingdom (GBR).
Hickey, R.L., Gerlach, D.C., Frey, F.A., 1984. Geochemical Variations in Volcanic Rocks from Central-South Chile (33–42 Degrees S). Shiva Publ., Nantwich, Nantwich, United Kingdom (GBR), pp. 72–95.
Hickey, R.L., Frey, F.A., Gerlach, D.C., Lopez-Escobar, L., 1986. Multiple sources for basaltic arc rocks from the Southern Volcanic Zone of the Andes (34 degrees−41 degrees S); trace element and isotopic evidence for contributions from subducted oceanic crust, mantle, and continental crust. Journal of Geophysical Research 91, 5963–5983.
Hickey-Vargas, R., Moreno Roa, H., Lopez-Escobar, L., Frey, F.A., 1989. Geochemical variations in Andean basaltic and silicic lavas from the Villarrica–Lanin volcanic chain (39.5 degrees S); an evaluation of source heterogeneity, fractional crystallization and crustal assimilation. Contributions to Mineralogy and Petrology 103, 361–386.
Hickey-Vargas, R., Abdollahi, M.J., Parada, M.A., Lopez-Escobar, L., Frey, F.A., 1995. Crustal xenoliths from Calbuco Volcano, Andean Southern Volcanic Zone; implications for crustal composition and magma-crust interaction. Contributions to Mineralogy and Petrology 119, 331–344.
Hickey-Vargas, R., Sun, M., Lopez-Escobar, L., Moreno-Roa, H., Reagan, M.K., Morris, J.D., Ryan, J.G., 2002. Multiple subduction components in the mantle wedge; evidence from eruptive centers in the central southern volcanic zone, Chile. Geology (Boulder) 30, 199–202.
Hickey-Vargas, R., Sun, M., Holbik, S., 2016. Geochemistry of basalts from small eruptive centers near Villarrica stratovolcano, Chile: evidence for lithospheric mantle components in continental arc magmas. Geochimica et Cosmochimica Acta http://dx.doi.org/10.1016/j.gca.2016.03.033.
Hildreth, W., Drake, R.E., 1992. Volcan Quizapu, Chilean Andes. Bulletin of Volcanology 54, 93–125.
Hildreth, W., Moorbath, S., 1988. Crustal contributions to arc magmatism in the Andes of central Chile. Contributions to Mineralogy and Petrology 98, 455–489.
Holbik, S., 2014. Arc Crust–Magma Interaction in the Andean Southern Volcanic Zone from Thermobarometry, Mineral Composition, Radiogenic Isotope and Rare Earth

Element Systematics of the Azufre–Planchon–Peteroa Volcanic Complex, Chile Ph.D. thesis Florida International University.
Holm, P.M., Soager, N., Dyhr, C.T., Nielsen, M.R., 2014. Enrichments of the mantle sources beneath the Southern Volcanic Zone (Andes) by fluids and melts derived from abraded upper continental crust. Contributions to Mineralogy and Petrology 167, 1–27.
Jacques, G., Hoernle, K., Gill, J., Hauff, F., Wehrmann, H., Garbe-Schönberg, D., van den Bogaard, P., Bindeman, I., Lara, L.E., 2013. Across-arc geochemical variations in the Southern Volcanic Zone, Chile (34.5–38.0°S): constraints on mantle wedge and slab input compositions. Geochimica et Cosmochimica Acta 123, 218–243.
Jacques, G., Hoernle, K., Gill, J., Wehrmann, H., Bindeman, I., Lara, L.E., 2014. Geochemical variations in the Central–Southern volcanic zone, Chile (38–43 degrees S); the role of fluids in generating arc magmas. Chemical Geology 371, 27–45.
Jicha, B.R., Singer, B.S., Brophy, J.G., Fournelle, J.H., Johnson, C.M., Beard, B.L., Lapen, T.J., Mahlen, N.J., 2004. Variable impact of the subducted slab on Aleutian island arc magma sources; evidence from Sr, Nd, Pb, and Hf isotopes and trace element abundances. Journal of Petrology 45, 1845–1875.
Jicha, B.R., Singer, B.S., Beard, B.L., Johnson, C.M., Moreno-Roa, H., Naranjo, J.A., 2007. Rapid magma ascent and generation of (super 230) Th excesses in the lower crust at Puyehue–Cordon Caulle, Southern Volcanic Zone, Chile. Earth and Planetary Science Letters 255, 229–242.
Kay, S.M., Godoy, E., Kurtz, A., 2005. Episodic arc migration, crustal thickening, subduction erosion, and magmatism in the south-central Andes. Geological Society of America Bulletin 117, 67–88.
Kimura, J., Hacker, B.R., van Keken, P.E., Kawabata, H., Yoshida, T., Stern, R.J., 2009. Arc Basalt Simulator version 2, a simulation for slab dehydration and fluid-fluxed mantle melting for arc basalts; modeling scheme and application. Geochemistry, Geophysics, Geosystems G3 (10) (Citation Q09004).
Lara, L.E., Naranjo, J.A., Moreno, H., 2004. Lanin Volcano (39.5 degrees S), Southern Andes; geology and morphostructural evolution. Revista Geologica de Chile 31, 241–257.
Lara, L.E., Moreno, H., Naranjo, J.A., Matthews, S., Perez de Arce, C., 2006a. Magmatic evolution of the Puyehue–Cordon Caulle volcanic complex (40 degrees S), Southern Andean Volcanic Zone; from shield to unusual rhyolitic fissure volcanism. Journal of Volcanology and Geothermal Research 157, 343–366.
Lara, L.E., Lavenu, A., Cembrano, J., Rodriguez, C., 2006b. Structural controls of volcanism in transversal chains; resheared faults and neotectonics in the Cordon Caulle–Puyehue area (40.5 degrees S), Southern Andes. Journal of Volcanology and Geothermal Research 158, 70–86.
Lee, C.-T.A., Luffi, P., Plank, T., Dalton, H., Leeman, W.P., 2009. Constraints on the depths and temperatures of basaltic magma generation on Earth and other terrestrial planets using new thermobarometers for mafic magmas. Earth and Planetary Science Letters 279, 20–33.
Lopez-Escobar, L., 1984. Petrology and Chemistry of Volcanic Rocks of the Southern Andes. Shiva Publ., Nantwich, Nantwich, United Kingdom (GBR), pp. 47–71.
Lopez-Escobar, L., Moreno, H., 1981. Erupcion de 1979 del volcan Mirador, Andes del Sur, 40 degrees 21'S.; Caracteristicas geoquimica de las lavas y xenolitos graniticos. Eruption in 1979 of the Mirador Volcano, Southern Andes; geochemical characteristics of the lavas and granitic inclusions. Revista Geologica de Chile 13 & 14, 17–33.
Lopez-Escobar, L., Moreno, R.,.H., 1994. Geochemical characteristics of the Southern Andes basaltic volcanism associated with the Liquiñe–Ofqui fault zone between 39 degrees and 46 degrees S. Actas - Congreso Geologico Chileno 7 (2), 1388–1393.
Lopez-Escobar, L., Kilian, R., Kempton, P.D., Tagiri, M., 1993. Petrography and geochemistry of Quaternary rocks from the Southern Volcanic Zone of the Andes between 41 degrees 30′ and 46 degrees 00′S, Chile. Revista Geologica de Chile 20, 33–55.
López-Escobar, L., Cembrano, J., Moreno, H., 1995a. Geochemistry and tectonics of the Southern Andes basaltic Quaternary volcanism associated with the Liquiñe–Ofqui Fault Zone, (37°–46°S). Revista Geológica de Chile 22, 219–234.
Lopez-Escobar, L., Parada, M.A., Hickey-Vargas, R., Frey, F.A., Kempton, P.D., Moreno, H., 1995b. Calbuco Volcano and minor eruptive centers distributed along the Liquiñe–Ofqui fault zone, Chile (41 degrees—42 degrees S); contrasting origin of andesitic and basaltic magma in the Southern Volcanic Zone of the Andes. Contributions to Mineralogy and Petrology 119, 345–361.
Lucassen, F., Trumbull, R., Franz, G., Creixell, C., Vasquez, P., Romer, R.L., Figueroa, O., 2004. Distinguishing crustal recycling and juvenile additions at active continental margins: the Paleozoic to recent compositional evolution of the Chilean Pacific margin (36-41°S). Journal of South American Earth Sciences 17, 103–119.
Lucassen, F., Wiedicke, M., Franz, G., 2010. Complete recycling of a magmatic arc: evidence from chemical and isotopic composition of Quaternary trench sediments in Chile (36°-40°S). International Journal of Earth Sciences 99, 687–701.
Mamani, M., Woerner, G., Sempere, T., 2010. Geochemical variations in igneous rocks of the Central Andean Orocline (13 degrees S to 18 degrees S); tracing crustal thickening and magma generation through time and space. Geological Society of America Bulletin 122, 162–182.
McMillan, N.J., Harmon, R.S., Moorbath, S., Lopez-Escobar, L., Strong, D.F., 1989. Crustal sources involved in continental arc magmatism; a case study of Volcan Mocho–Choshuenco, southern Chile. Geology (Boulder) 17, 1152–1156.
Morris, J.D., Leeman, W.P., Tera, F., 1990. The subducted component in island arc lavas; constraints from B-Be isotopes and Be systematics. Nature (London) 344, 31–36.
Muntener, O., Kelemen, P., Grove, T.L., 2001. The role of H_2O during crystallization of primitive arc magmas. Earth and Planetary Science Letters 279, 20–33.
Naranjo, J.A., Stern, C.R., 1998. Holocene explosive activity of Hudson Volcano, southern Andes. Bulletin of Volcanology 59, 291–306.
Parada, M.A., Lopez-Escobar, L., Oliveros, V., Fuentes, F., Morata, D., Calderon, M., Aguirre, L., Feraud, G., Espinoza, F., Moreno, H., Figueroa, O., Munoz Bravo, J., Troncosco Vasquez, R., Stern, C.R., 2007. Andean Magmatism. The Geological Society, London, London, United Kingdom (GBR).
Plank, T., Langmuir, C.H., 1988. An evaluation of the global variations in the major element chemistry of arc basalts. Earth and Planetary Science Letters 90, 349–370.
Plank, T., Langmuir, C.H., 1993. Tracing trace elements from sediment input to volcanic output at subduction zones. Nature (London) 362, 739–743.
Reagan, M.K., Sims, K.W.W., Erich, J., Thomas, R.B., Cheng, H., Edwards, R.L., Layne, G., Ball, L., 2003. Time-scales of differentiation from mafic parents to rhyolite in north American continental arcs. Journal of Petrology 44, 1703–1726.
Reubi, O., Bourdon, B., Dungan, M.A., Koornneef, J.M., Selles, D., Langmuir, C.H., Aciego, S., 2011. Assimilation of the plutonic roots of the Andean arc controls variations in U-series disequilibria at Volcan Llaima, Chile. Earth and Planetary Science Letters 303, 37–47.
Rodríguez, C. 1999. Geoquímica del Grupo Carrán–Los Venados, Andes del Sur (40.3°S). Universidad de Chile, thesis (unpublished). 133 pp. Santiago.
Rodriguez, C., Selles, D., Dungan, M., Langmuir, C.H., Leeman, W., 2007. Adakitic dacites formed by intracrustal crystal fractionation of water-rich parent magmas at Nevado de Longavi Volcano (36.2 degrees S; Andean Southern Volcanic Zone, central Chile). Journal of Petrology 48, 2033–2061.
Ruprecht, P., Cooper, K., 2012. Integrating the uranium-series and elemental diffusion geochronometers in mixed magmas from volcan Quizapu, Central Chile. Journal of Petrology 53, 841–871.
Ruprecht, P., Bergantz, G.W., Cooper, K.M., Hildreth, W., 2012. The crustal magma storage sytem of volcan Quizapu, Chile, and the effects of magma mixing on magma diversity. Journal of Petrology 53, 801–840.
Salters, V.J.M., Mallick, S., Hart, S.R., Langmuir, C.E., Stracke, A., 2011. Domains of depleted mantle: new evidence from hafnium and neodymium isotopes. Geochemistry, Geophysics, Geosystems 12. http://dx.doi.org/10.1029/2011GC003617.
Schindlbeck, J.C., Freundt, A., Kutterolf, S., 2014. Major changes in the post-glacial evolution of magmatic compositions and pre-eruptive conditions of Llaima Volcano, Andean Southern Volcanic Zone, Chile. Bulletin of Volcanology 76, 1–22.
Selles, D., Rodriguez, A.C., Dungan, M.A., Naranjo, J.A., Gardeweg, M., 2004. Geochemistry of Nevado de Longavi Volcano (36.2 degrees S); a compositionally atypical arc volcano in the Southern Volcanic Zone of the Andes. Revista Geologica de Chile 31, 293–315.
Sigmarsson, O., Condomines, M., Morris, J.D., Harmon, R.S., 1990. Uranium and ^{10}Be enrichments by fluids in Andean arc magmas. Nature (London) 346, 163–165.
Sigmarsson, O., Chmeleff, J., Morris, J., Lopez-Escobar, L., 2002. Origin of (super 226) Ra-(super 230) Th disequilibria in arc lavas from Southern Chile and implications for magma transfer time. Earth and Planetary Science Letters 196, 189–196.
Singer, B.S., Leeman, W.P., Thirlwall, M.F., Rogers, N.W., 1996. Does fracture zone subduction increase sediment flux and mantle melting in subduction zones? Trace element evidence from Aleutian Arc basalt. Geophysical Monograph 96, 285–291.
Singer, B.S., Thompson, R.A., Dungan, M.A., Feeley, T.C., Nelson, S.T., Pickens, J.C., Brown, L.L., Wulff, A.W., Davidson, J.P., Metzger, J., 1997. Volcanism and erosion during the past 930 k.y. at the Tatara-San Pedro complex, Chilean Andes. Geological Society of America Bulletin 109, 127–142.
Singer, B.S., Jicha, B.R., Harper, M.A., Naranjo, J.A., Lara, L.E., Moreno-Roa, H., 2008. Eruptive history, geochronology, and magmatic evolution of the Puyehue-cordon Caulle volcanic complex, Chile. Geological Society of America Bulletin 120, 599–618.
Sruoga, P., Llambias, E.J., Fauque, L., Schonwandt, D., Repol, D.G., 2005. Volcanological and geochemical evolution of the Diamante Caldera–Maipo volcano complex in the southern Andes of Argentina (34 degrees 10′S). Journal of South American Earth Sciences 19, 399–414.
Sruoga, P., Etcheverria, M.P., Feineman, M., Rosas, M., Burkert, C., Ibanes, O., 2012. Complejo Caldera Diamante–Volcan Maipo (34 degrees 10′S, 69 degrees 50′W) evolucion volcanologica y geoquimica e implicancias en su peligrosidad. Revista de la Asociacion Geologica Argentina 69, 508–530.
Stern, C.R., 2011. Subduction erosion; rates, mechanisms, and its role in arc magmatism and the evolution of the continental crust and mantle. Gondwana Research 20, 284–308.
Stern, C.R., Naranjo, J.A., 2015. Along arc petrochemical variations in the southernmost Andean SVZ (43.5–46°S): implications for magma genesis. Expanded Abstracts XIV Congreso Geologico de Chile, La Serena, October 4–8, 2015.
Stern, C.R., Futa, K., Muehlenbachs, K., Dobbs, F.M., Munoz, J., Godoy, E., Charrier, R., 1984. Sr, Nd, Pb and O Isotope Composition of Late Cenozoic Volcanics, Northernmost SVZ (33–34 Degrees S). Shiva Publ., Nantwich, Nantwich, United Kingdom (GBR), pp. 96–105.
Stern, C.R., Frey, F.A., Futa, K., Zartman, R.E., Peng, Z., Kyser, T.K., 1990. Trace-element and Sr, Nd, Pb and O isotopic composition of Pliocene and Quaternary alkali basalts of the Patagonian plateau lavas of southernmost South America. Contributions to Mineralogy and Petrology 104, 294–308.
Stern, C.R., Moreno, H., Lopez-Escobar, L., Clavero, J.E., Lara, L.E., Naranjo, J.A., Parada, M.A., Skewes, M.A., 2007. Chilean Volcanoes. The Geological Society, London, London, United Kingdom (GBR).
Stracke, A., Bourdon, B., McKenzie, D., 2006. Melt extraction in the Earth's mantle: constraints from U–Th–Pa–Ra studies in oceanic basalts. Earth and Planetary Science Letters 244, 97–112.
Tassara, A., Echaurren, A., 2012. Anatomy of the Andean subduction zone; three-dimensional density model upgraded and compared against global-scale models. Geophysical Journal International 189, 161–168.
Tassara, A., Goetze, H., Schmidt, S., Hackney, R., 2006. Three-dimensional density model of the Nazca Plate and the Andean continental margin. Journal of Geophysical Research 111, B09404. http://dx.doi.org/10.1029/2005JB003976.
Tebbens, S.F., Cande, S.C., Kovacs, L., Parra, J.C., LaBrecque, J.L., Vergara, H., 1997. The Chile ridge: a tectonic framework. Journal of Geophysical Research 102, 12035–12059.

Thorpe, R.S., 1984. The Tectonic Setting of Active Andean Volcanism. Shiva Publ., Nantwich, Nantwich, United Kingdom (GBR), pp. 4–8.
Thorwart, M., Dzierma, Y., Lieser, K., Buhs, H., Rabbel, W., 2014. Shear-wave velocity structure of the Chilean subduction zone (39–40 degrees S) based on Rayleigh wave dispersion; evidence of fluid release and melts in the mantle beneath the Villarrica Volcano. Special Publication - Geological Society of London 410, 59–70.
Tormey, D.R., Hickey-Vargas, R., Frey, R.A., Lopez-Escobar, L., Harmon, R.S., Rapela, C.W., 1991a. Recent lavas from the Andean volcanic front (33–42 degrees S); interpretations of along-arc compositional variations. Special Paper - Geological Society of America 265, 57–77.
Tormey, D., Schuller, P., Lopez-Escobar, L., Frey, F., 1991b. Uranium-thorium activities and disequilibrium in volcanic rocks from the Andes (33–46 degrees S); petrogenetic constraints and environmental consequences. Revista Geologica de Chile 18, 165–176.
Tormey, D.R., Frey, F.A., Lopez-Escobar, L., 1995. Geochemistry of the active Azufre–Planchon–Peteroa volcanic complex, Chile (35 degrees 15′S); evidence for multiple sources and processes in a cordilleran arc magmatic system. Journal of Petrology 36, 265–298.
Turner, S.J., Langmuir, C., 2015a. What processes control the chemical compositions of arc-front stratovolcanoes? Geochemistry, Geophysics, Geosystems 16. http://dx.doi.org/10.1002/2014GC005633.
Turner, S.J., Langmuir, C.H., 2015b. The global chemical systematics of arc front stratovolcanoes; evaluating the role of crustal processes. Earth and Planetary Science Letters 422, 182–193.
Turner, S., Bourdon, B., Gill, J., 2003. Insights into magma genesis at convergent margins from U-series isotopes uranium-series geochemistry. Reviews of Mineralogy and Geochemistry 52, 255–315.
Turner, S., Regelous, M., Hawkesworth, C., Rostami, K., 2006. Partial melting processes above subducting plates: constraints from 231 Pa–235 U disequilibria. Geochimica et Cosmochimica Acta 70, 480–503.
Vervoort, J.D., Plank, T., Prytulak, J., 2011. The Hf–Nd isotopic composition of marine sediments. Geochimica et Cosmochimica Acta 75, 5903–5926.
Voelker, D., Kutterolf, S., Wehrmann, H., 2011. Comparative mass balance of volcanic edifices at the Southern Volcanic Zone of the Andes between 33 degrees S and 46 degrees S. Journal of Volcanology and Geothermal Research 205, 114–129.
Voelker, D., Geersen, J., Contreras-Reyes, E., Sellanes, J., Pantoja, S., Rabbel, W., Thorwart, M., Reichert, C., Block, M., Weinrebe, W.R., 2013. Morphology and geology of the continental shelf and upper slope of southern central Chile (33 degrees S-43 degrees S). International Journal of Earth Sciences = Geologische Rundschau 103, 1765–1787.
Watt, S.F.L., Pyle, D.M., Mather, T.A., 2011a. Geology, petrology and geochemistry of the dome complex of Huequi Volcano, southern Chile. Andean Geology 38, 335–348.
Watt, S.F.L., Pyle, D.M., Naranjo, J.A., Rosqvist, G., Mella, M., Mather, T.A., Moreno, H., 2011b. Holocene tephrochronology of the Hualaihue region (Andean Southern Volcanic Zone, approximately 42 degrees S), southern Chile. Quaternary International 246, 324–343.
Watt, S.F., Pyle, D.M., Mather, T.A., Naranjo, J.A., 2013. Arc magma compositions controlled by linked thermal and chemical gradients above the subducting slab. Geophysical Research Letters 40, 72–78.
Wehrmann, H., Hoernle, K., Garbe-Schoenberg, D., Jacques, G., Mahlke, J., Schumann, K., 2014. Insights from trace element geochemistry as to the roles of subduction zone geometry and subduction input on the chemistry of arc magmas. International Journal of Earth Sciences = Geologische Rundschau 103, 1929–1944.